From Graphene to Graphite to Nanotubes to Graphene

Mildred Dresselhaus

Massachusetts Institute of Technology

Cambridge, MA

APS March Meeting Graphene Tutorial

New Orleans

March 9, 2008

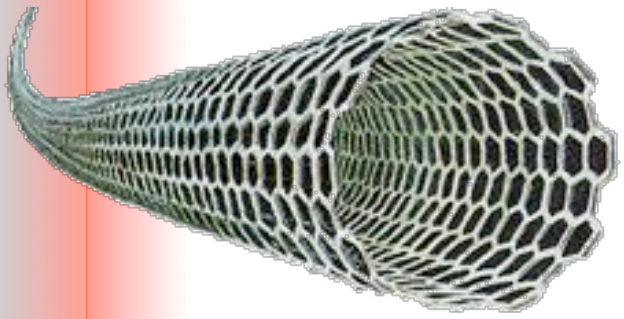

Collaborators:

G. Dresselhaus, MIT
H. Son, MIT
J. Kong, MIT
M. Hofmann, MIT
L.G. Cancado, Rochester
G.G. Samsonidze, UC Berkeley
M.A. Pimenta, UFMG Brazil
A. Jorio, UFMG Brazil
F. Plentz Filho, UFMG Brazil
A. Souza Filho, UFC Brazil
R. Capaz, UFRJ Brazil
Paula Corio, USP Brazil
M. Endo, Shinshu U
R. Saito, Tohoku U
J. Jiang, Tohoku U
Y.A. Kim, Shinshu U
M. Terrones, IPICYT, Mexico

Outline

- Historical Graphene to Graphene path
- Carbon Nanotubes as Prototype Materials
- Disordered Graphite
- Graphene and Graphene Ribbons
- Looking to the Future of Carbon Nanostructures

Graphene is the Mother of all nano-Graphitic forms

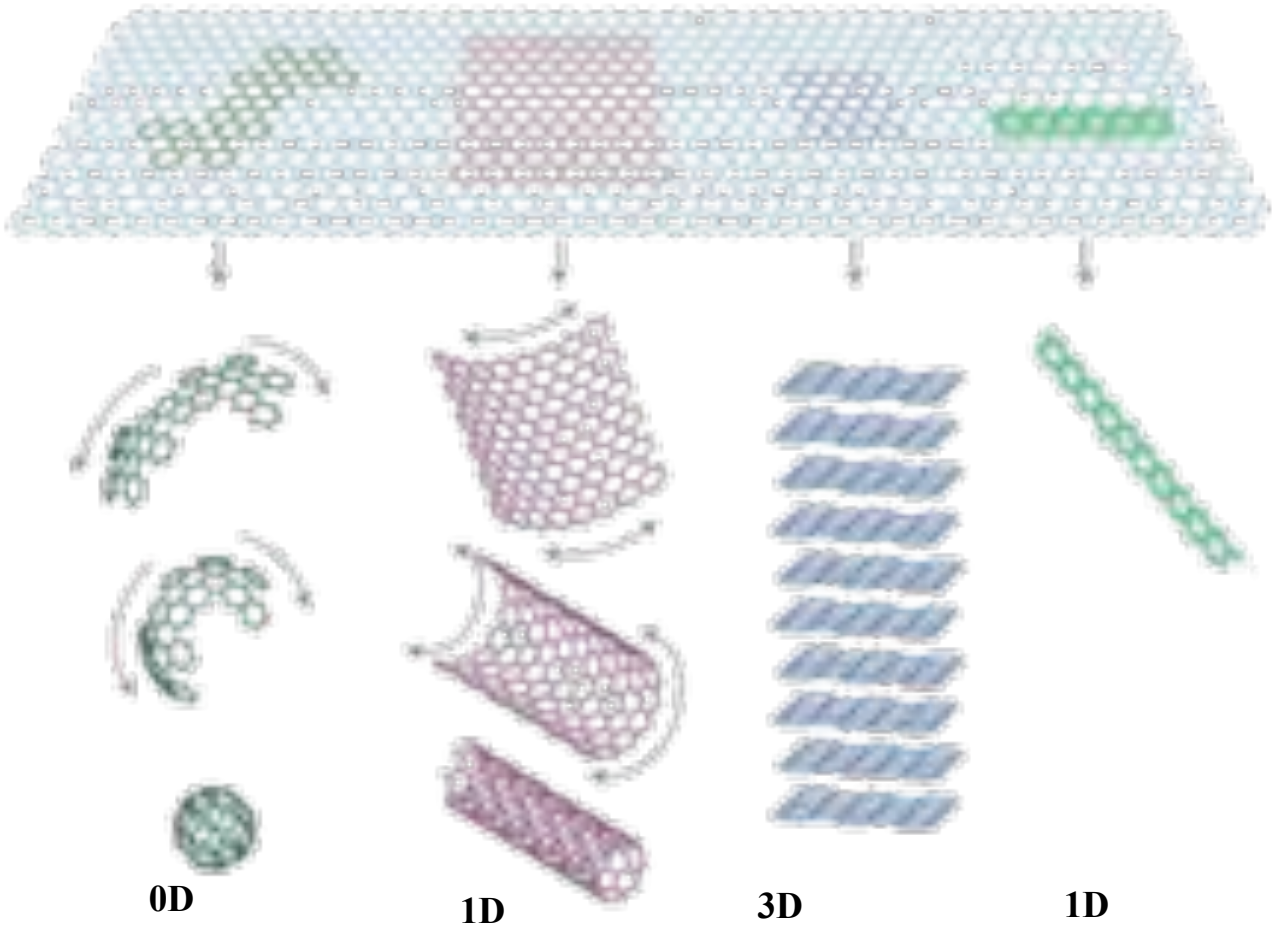

- A graphene sheet is one million times thinner (10^{-6}) than a sheet of paper.
- Graphene is a 2D building block material for other sp^2 bonded carbon materials. It can be wrapped up into 0D fullerenes, rolled into 1D nanotubes, cut into 1D graphene ribbons or stacked into 3D graphite

From graphene to graphite to fullerenes to nanotubes to graphene

In the opening overview, we follow a path:

- from the early work on graphene
- to the developments in graphite
- to graphite intercalation compounds
- to fullerenes
- to nanotubes
- and then back to graphene

The Electronic Structure of Graphene is the starting point for the electronic structure of graphite

P.R. Wallace, Phys. Rev. **71**, 622 (1947)

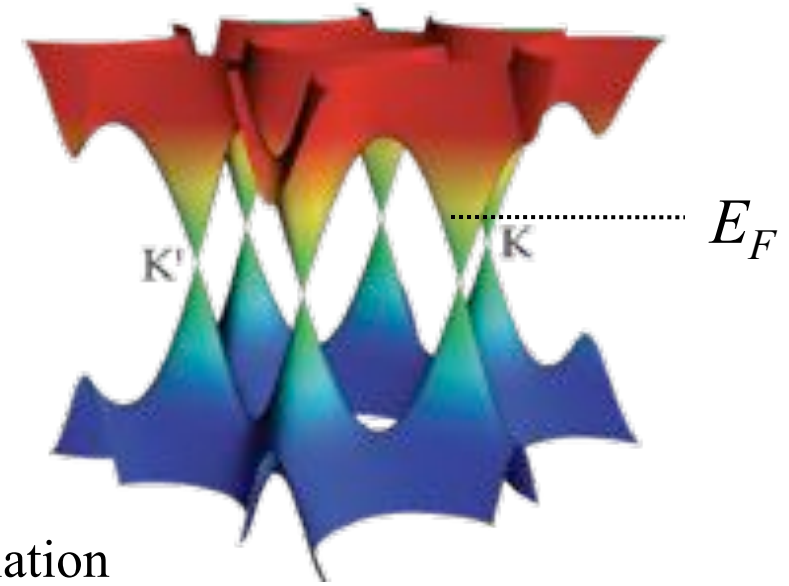

Near the K point

linear κ relation

where and

and is the overlap integral between nearest neighbor π-orbitals

(γ_0 values are from 2.9 to 3.1eV)

2D Graphite (Graphene) unit cells

Direct lattice

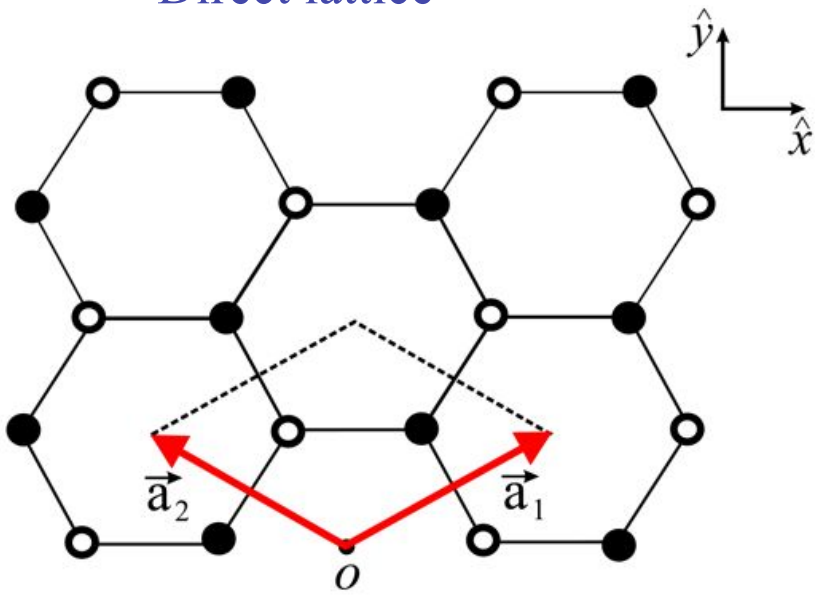

First Brillouin zone (BZ)

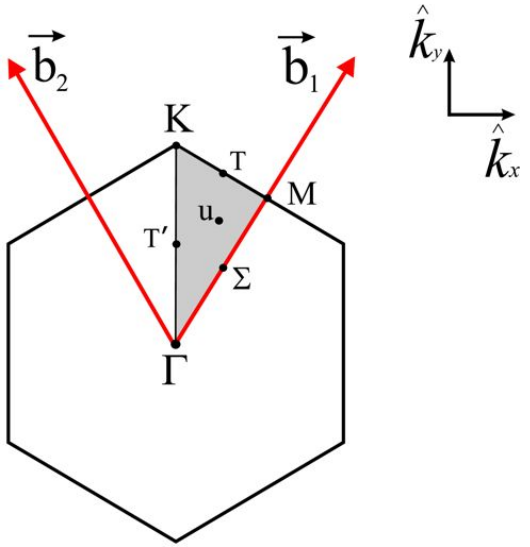

$$\vec{a}_1 = \frac{a}{2}\left(\sqrt{3}\,\hat{x} + \hat{y}\right)$$

$$\vec{a}_2 = \frac{a}{2}\left(-\sqrt{3}\,\hat{x} + \hat{y}\right)$$

$$a = 2.456\ \text{Å}$$

$$\vec{b}_1 = \frac{2\pi}{a}\left(\frac{\sqrt{3}}{3}\,\hat{k}_x + \hat{k}_y\right)$$

$$\vec{b}_2 = \frac{2\pi}{a}\left(-\frac{\sqrt{3}}{3}\,\hat{k}_x + \hat{k}_y\right)$$

Energy bands of 2D Graphite (graphene)

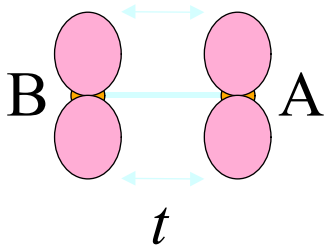

P. R. Wallace, *Phys. Rev*, **71** 622 (1947).

- π bands of graphene
  - Unit Cell, B. Z.
- Graphene is a zero gap semiconductor

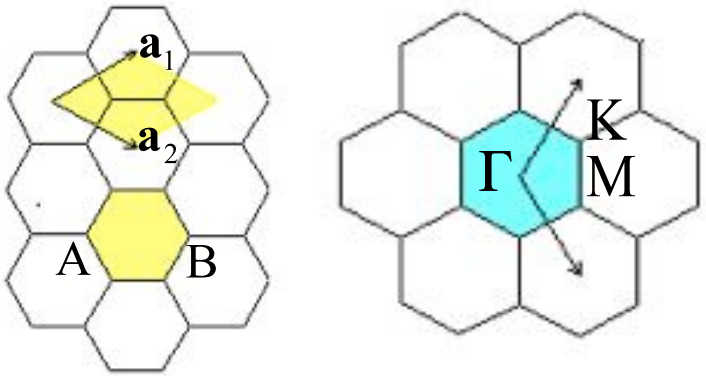

$$\mathbf{a}_1 = (\frac{\sqrt{3}}{2}, \frac{1}{2})a, \mathbf{a}_2 = (\frac{\sqrt{3}}{2}, -\frac{1}{2})a$$

$$\mathbf{b}_1 = (\frac{1}{2}, \frac{\sqrt{3}}{2})\frac{4\pi}{\sqrt{3}a}, \mathbf{b}_2 = (\frac{1}{2}, -\frac{\sqrt{3}}{2})\frac{4\pi}{\sqrt{3}a}$$

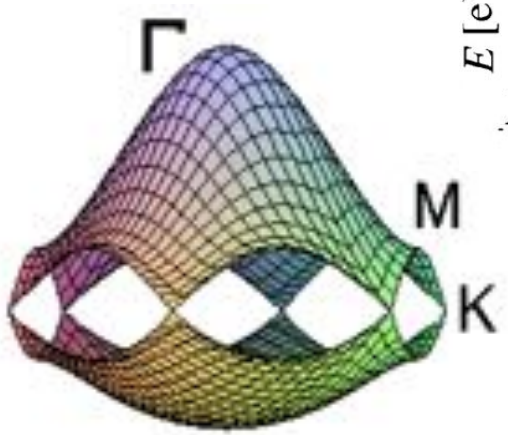

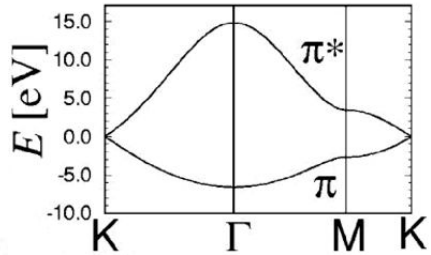

$$E_k = \pm t\sqrt{1 \pm 4\cos\frac{k_y a}{2}\cos\frac{\sqrt{3}k_x a}{2} + 4\cos^2\frac{k_y a}{2}}$$

3D Graphite

4 atoms/unit cell

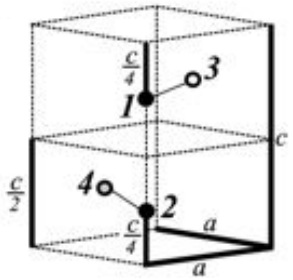

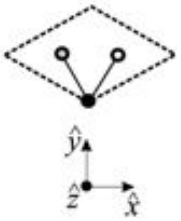

Direct lattice

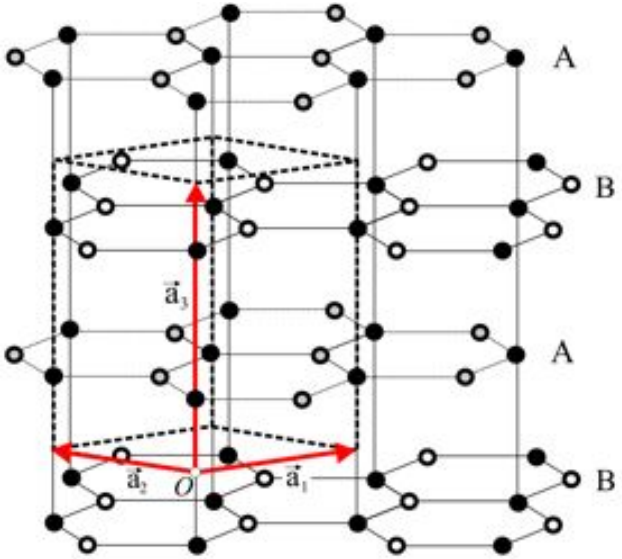

AB layer stacking

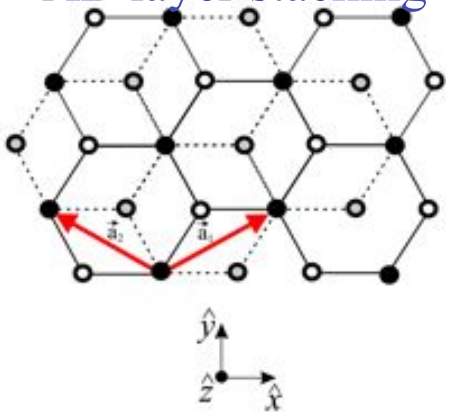

$$\vec{a}_1 = \frac{a}{2}\left(\sqrt{3}\,\hat{x} + \hat{y}\right)$$

$$\vec{a}_2 = \frac{a}{2}\left(-\sqrt{3}\,\hat{x} + \hat{y}\right)$$

$$\vec{a}_3 = c\,\hat{z}$$

$$a = 2.456\ \text{Å}$$

$$c = 6.6708\ \text{Å}$$

First Brillouin zone

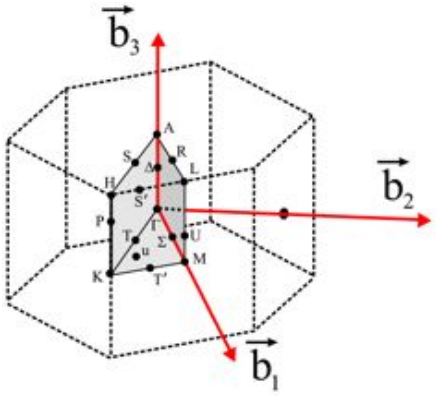

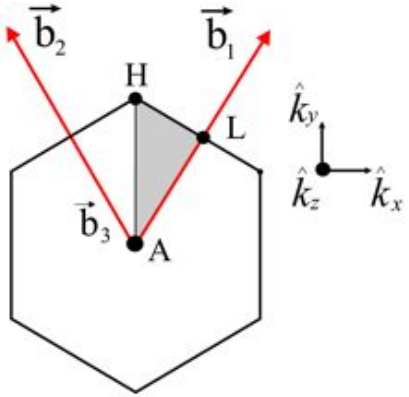

$$\vec{b}_1 = \frac{2\pi}{a}\left(\frac{\sqrt{3}}{3}\,\hat{k}_x + \hat{k}_y\right)$$

$$\vec{b}_2 = \frac{2\pi}{a}\left(-\frac{\sqrt{3}}{3}\,\hat{k}_x + \hat{k}_y\right)$$

$$\vec{b}_3 = \frac{2\pi}{c}\,\hat{k}_z$$

Extension of Graphene to Graphite

- McClure extended 2D graphene electronic structure calculation to 3D graphite.
- Magneto-optical experiment measured energy bands of graphite at several regions of the Brillouin zone

(near K and H)

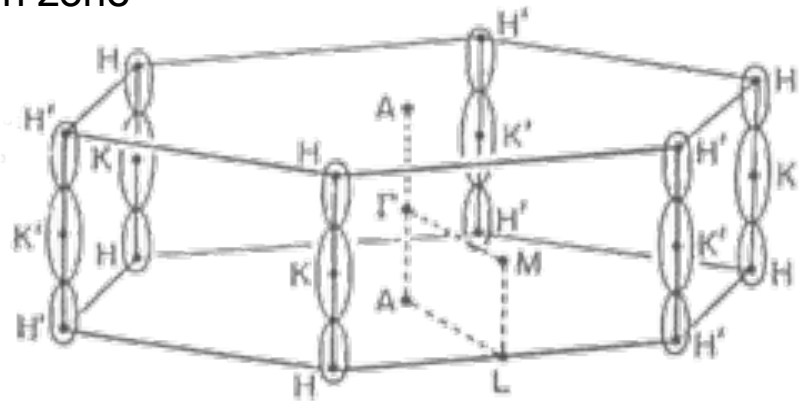

M.S. Dresselhaus and J.G. Mavroides. IBM Journal of Research and Development **8**, 262 (1964)

- Experiment (1961) was enabled by the availability of a new material, highly oriented pyrolytic graphite (HOPG) Ubbelohde (1960)
- Used symmetry-based E(k) model of McClure to yield band parameters for the electronic structure of graphite.

J.W. McClure, Phys. Rev. **108**, 612 (1957); **119**, 606 (1960)

Identification of Electrons and Holes in Graphite

Using circular polarized radiation in the first magneto-optical experiment to use a laser, the locations of electrons and holes in the Brillouin zone were identified

Experiment showed that electrons were located near K (K')

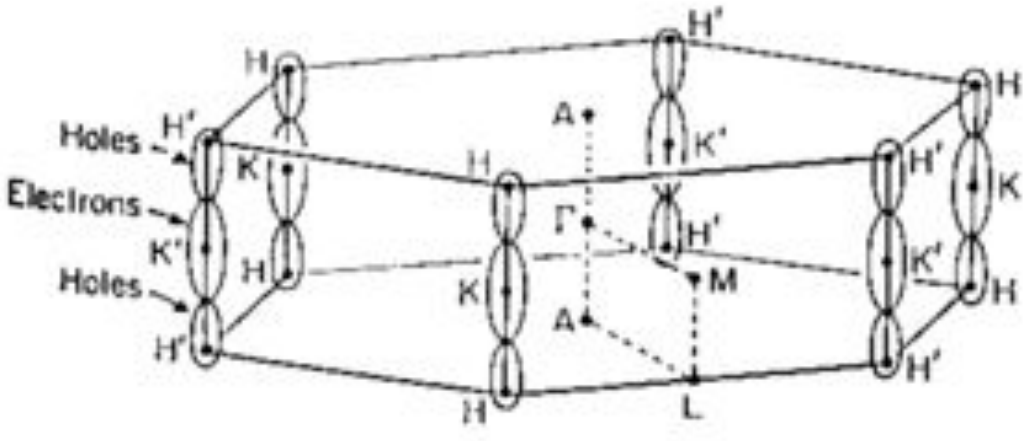

P.R.Schroeder, M.S. Dresselhaus and A.Javan, **Phys.Rev. Lett** 20,1292 (1968)

The locations of electrons and holes are incorrectly given in the literature, prior to 1968. The effective masses for electrons and holes in graphite are often used in the current graphene literature.

Spintronics in Graphene

- An early paper by Gene Dresselhaus defined what is now known as the "Dresselhaus spin-orbit term" in III-V semiconductors {G. Dresselhaus, **Phys. Rev**. 71, 220 (1955)} with *E(k)* having a linear *k*-dependence. A model for the spin-orbit interaction in graphite as imposed by symmetry was developed {G. Dresselhaus & M.S. Dresselhaus, **Phys. Rev**. 140, A401 (1965)}

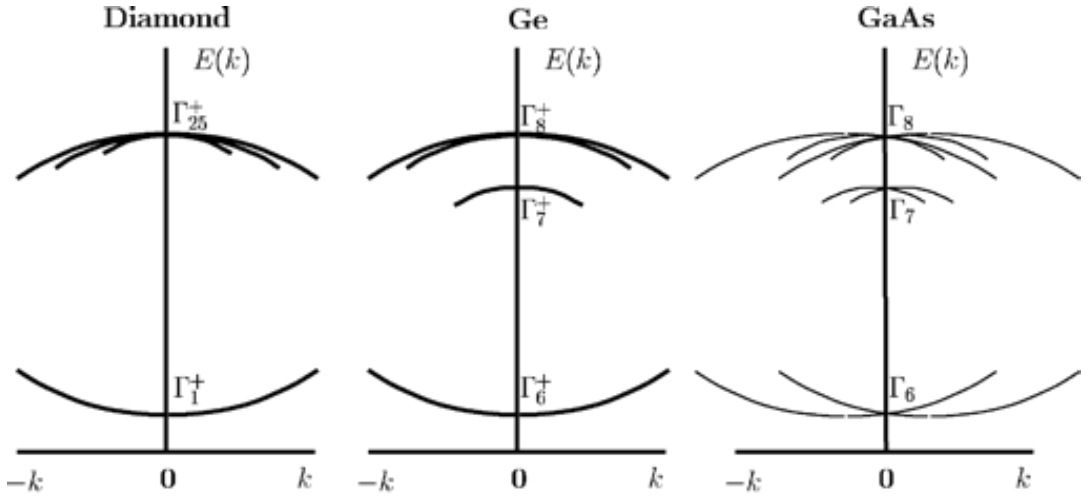

- Since the spin-orbit interaction in graphite is very small, the spin lifetime in graphene can be very long. Therefore graphene has become an interesting material for studying spin transport.

Entry into the Nanoworld

- Through the unexpected observation by Hannay et al. at AT&T Bell Labs of superconductivity in stage 1 graphite intercalation compounds (C_8K) (Hannay et al, **Phys.Rev.Lett.** 14, 225 (1965) much interest was aroused since neither potassium nor carbon is superconducting

- Intercalation compounds allowed early studies to be made of individual or few graphene layers in the environment of the intercalant species.

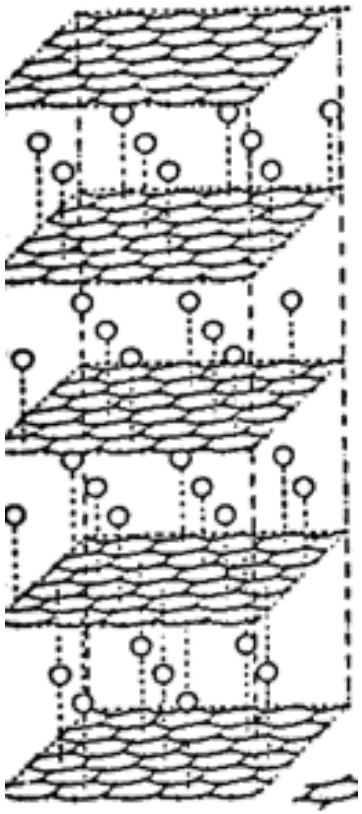

C_8K

Low Dimensional Science Studies in Graphite Intercalation Compounds (1973-1993)

Magnetoreflection

Transport

Raman

Optical

Structural

Magnetic

Superconductivity

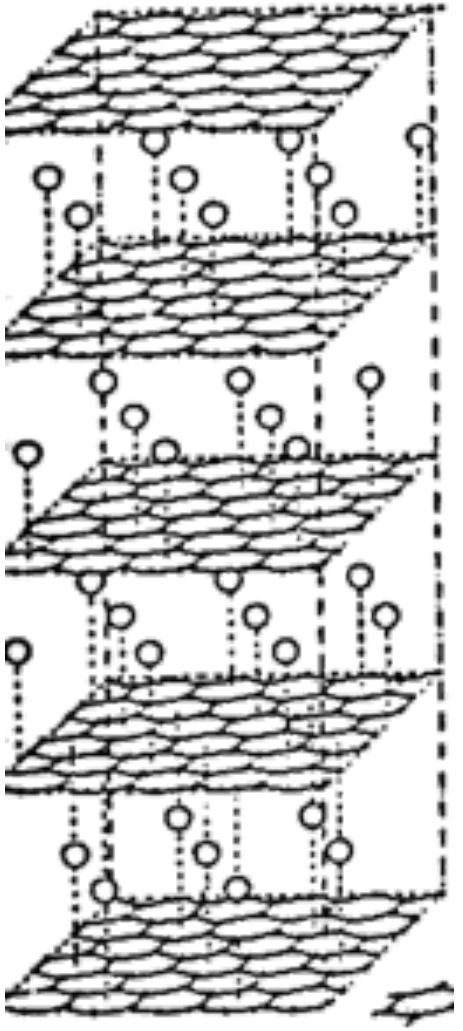

Studies on single or few layer Graphene were carried out in the environment of the intercalant species were carried out by many researchers

Concurrent Studies on Forerunners to Fullerenes

Intercalation led to ion implantation and laser irradiation of graphite

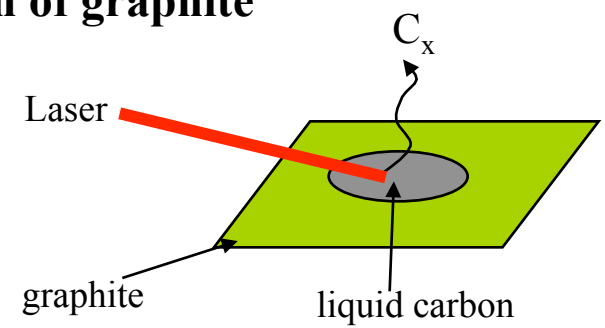

- Liquid carbon studies (1983)

  Liquid carbon was found to be metallic

  T. Venkatesan et al, Phys. Rev. Lett. 53, 360 (1984)

- The Laser ablation process used to make liquid carbon produced large clusters (like C_{100}) rather than C_2 or C_3

- Trip to Exxon Research Lab to discuss results.
- Soon Exxon published famous result showing mass spectroscopy intensity vs numbers of C atoms in clusters with peaks at C_{60} and C_{70}
- The Exxon result led to the discovery of fullerenes by Kroto, Smalley and Curl (1985)

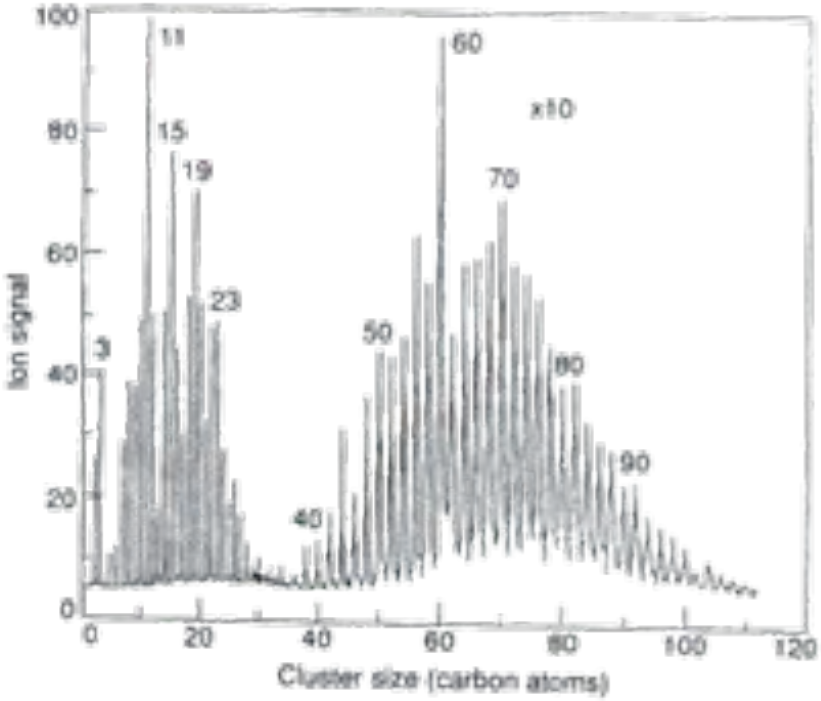

E.A.Rohlfing, D.M. Cox and A.Kaldor. J. Chem.Phys., 81, 332 (1984)

Forerunners of Carbon Nanotubes

- Vapor grown carbon fibers
- At center of these carbon fibers is a multiwall carbon nanotube
- A connection between fullerenes and nanotubes was made by going from $C_{60} \rightarrow C_{70} \rightarrow C_{80} \rightarrow$ nanotubes
- This idea suggested that a single wall Carbon nanotube would be interesting (August 1991) and led to calculating the electronic structure of SWNTs before they were ever seen

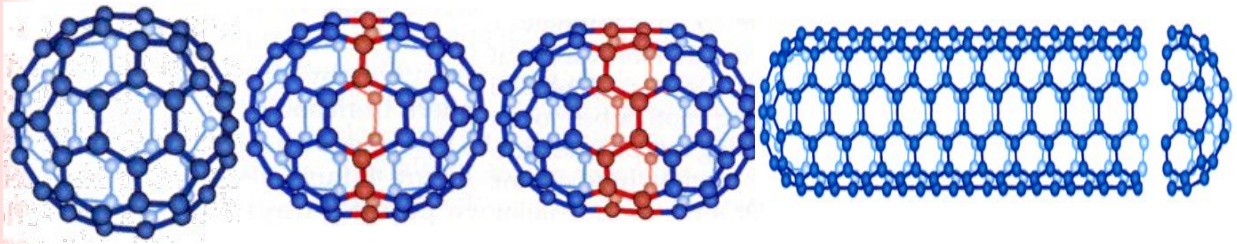

C_{60} C_{70} C_{80} CNT

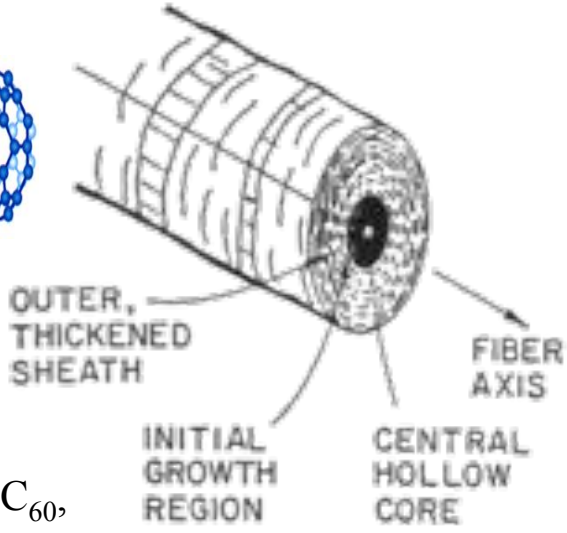

M.S.Dresselhaus et al., Graphite Fibers and Filaments, Springer (1988)
Saito, Fujita, Dresselhaus[2], Electronic structure of carbon fibers based on C_{60}, PRB 46, 1804 (1992)

Unique One Dimensional (1D) Properties

Carbon nanotubes and nanoribbons have:

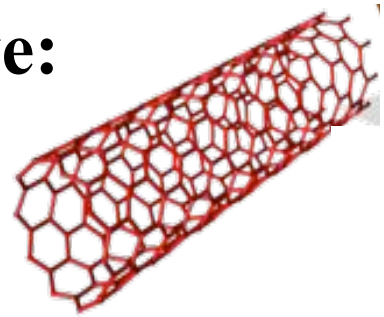

- **High aspect ratio**
- **Enhanced density of states in 1D**
- **Molecular behavior (spikes in DOS)**
- **Solid state behavior (tails in DOS)**

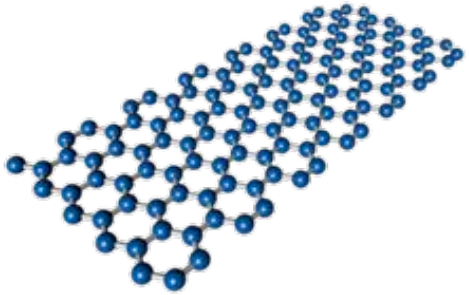

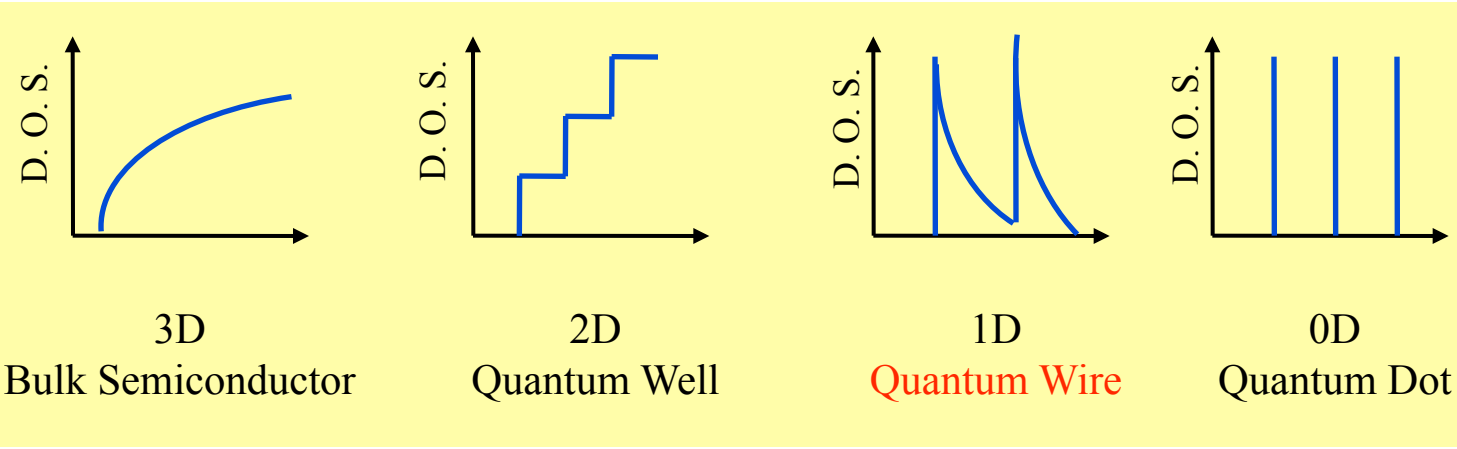

General Relations between 1D and 2D Systems shown in terms of carbon nanotubes

Rolling up a 2D sheet

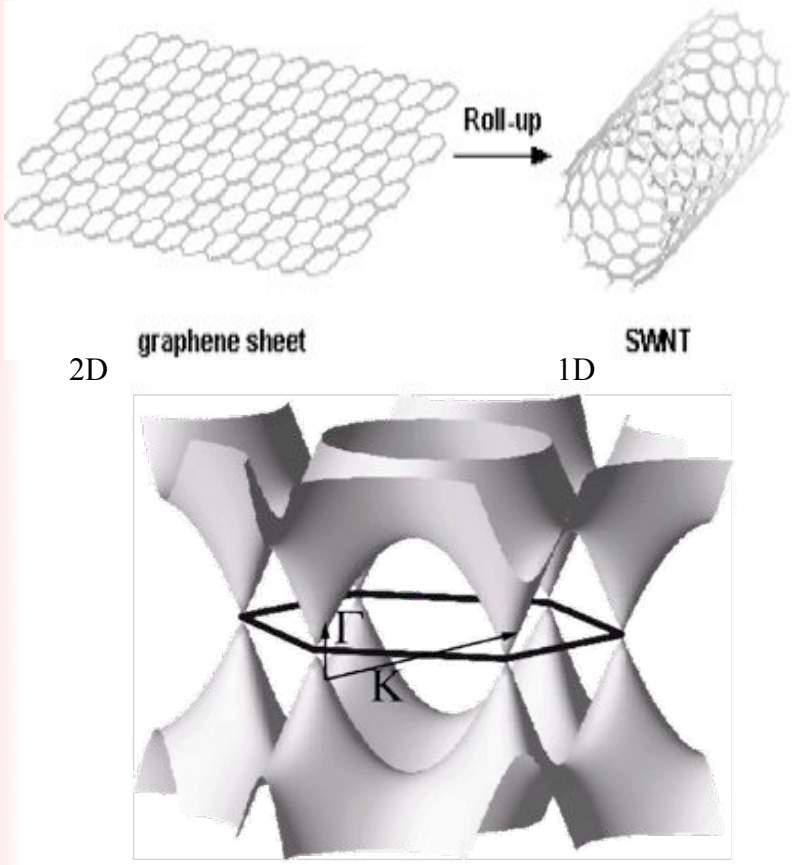

Confinement of 1D electronic states on **cutting lines**

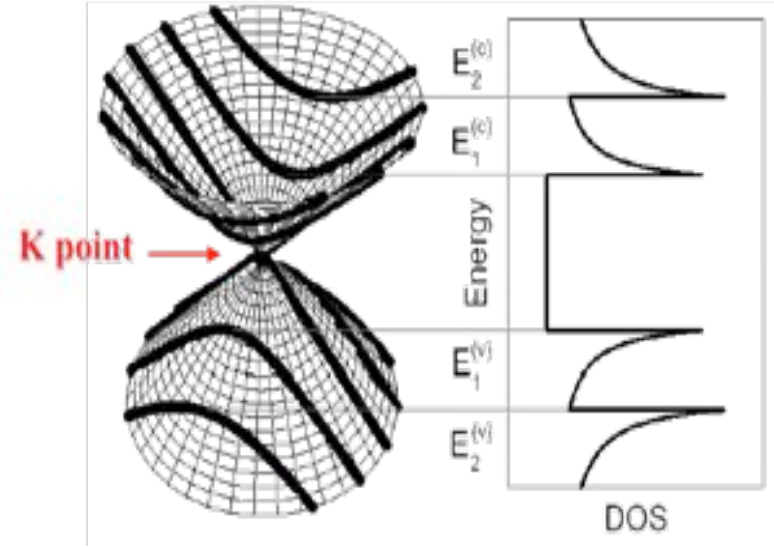

1D van Hove singularities give high density of electronic states (DOS) at well defined energies

- Carbon nanotubes are metallic if cutting line passes through the K point
- Otherwise they are semiconducting

Unique Properties of Carbon Nanotubes within the Nanoworld

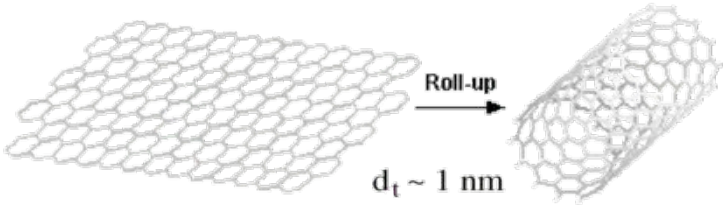

graphene ribbon **SWNT**

armchair

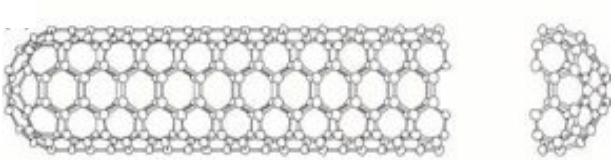

zigzag

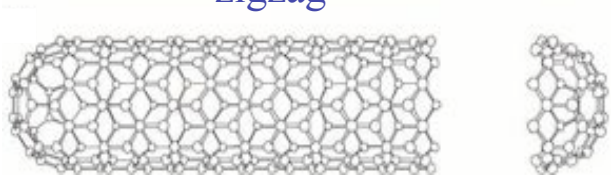

chiral

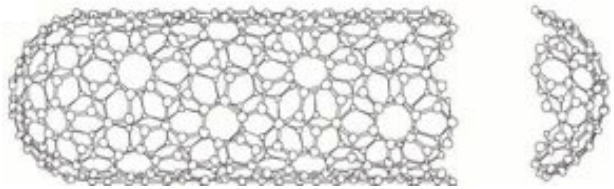

- Small size: ~1 nm diameter (down to ~10 atoms around the circumference)
- Electronic Properties: can be either metallic or semiconducting depending on diameter and orientation of the hexagons
- Mechanical: Very high strength, modulus, and resiliency.
- Physics: model system for1D density of electronic states.
- Single molecule Raman spectroscopy, luminescence and transport properties.

Outline

- Historical Graphene to Graphene path
- Carbon Nanotubes as Prototype Materials
- Disordered Graphite
- Graphene and Graphene Ribbons
- Looking to the Future of Carbon Nanostructures

Nanotube Structure in a Nutshell

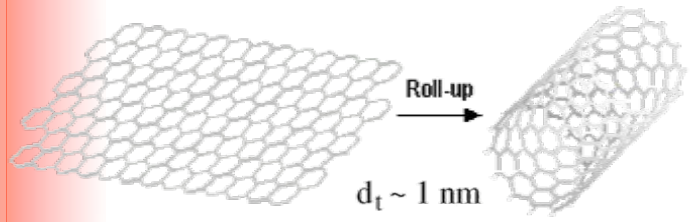

Graphene Sheet **SWNT**

Rolled-up graphene layer with a large unit cell.

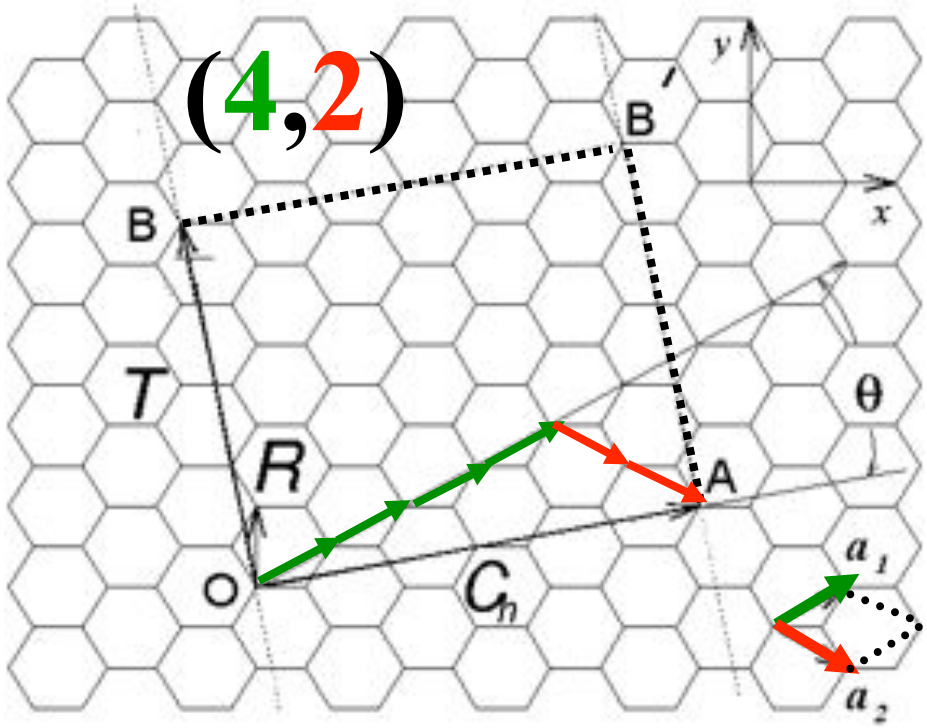

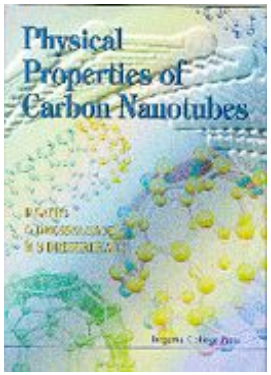

Each (n,m) nanotube is a unique molecule

R.Saito et al, Imperial College Press, 1998

Carbon Nanotubes

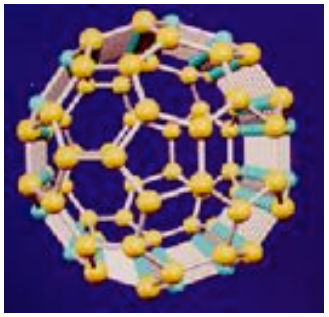

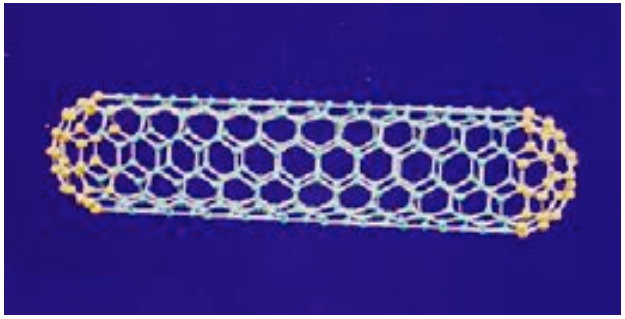

(5,5)

Armchair Nanotube

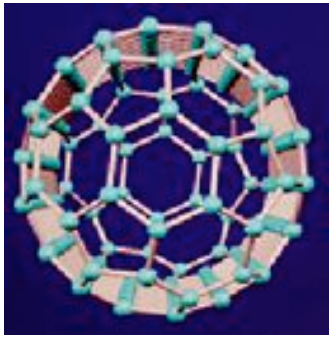

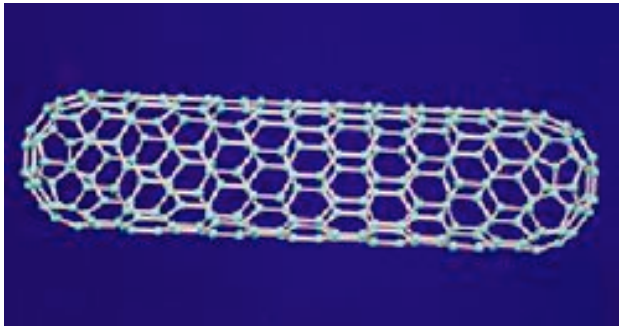

(9,0)

Zigzag Nanotube

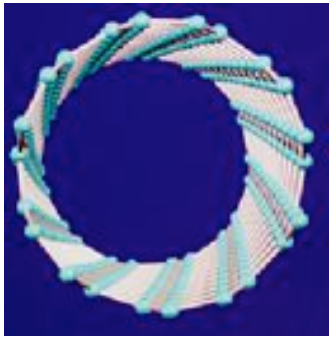

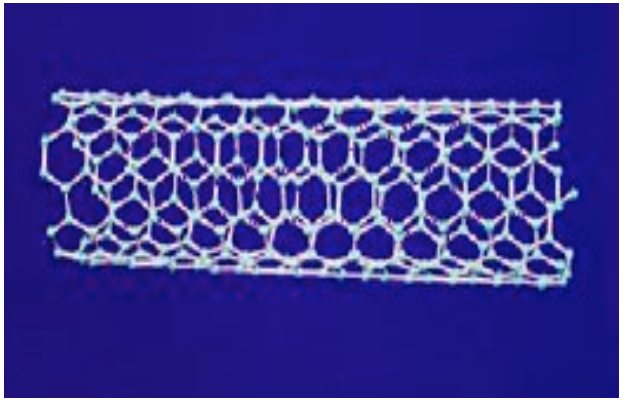

(6,5)

Chiral Nanotube

Hemispherical fullerene caps are shown for armchair and zigzag nanotubes

Energy Bands of Nanotubes

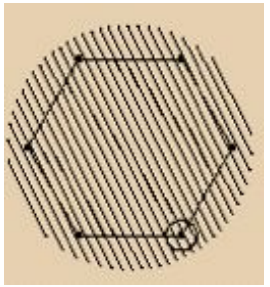

R. Saito *et al., Phys. Rev.* **B46**, 1804 (1992)

- *N* one-dimensional electronic energy bands

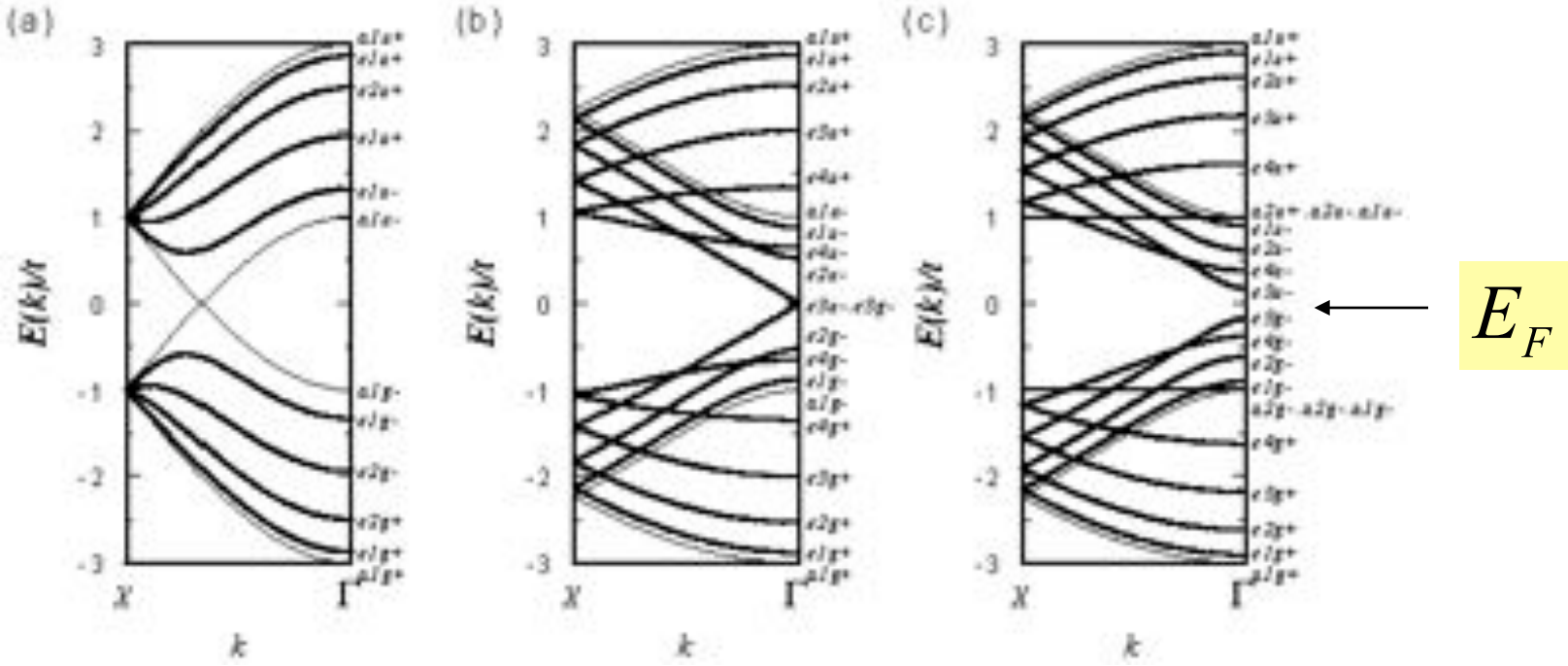

(5,5) (9,0) (10,0)

Metallic Carbon Nanotubes

R. Saito *et al, Phys. Rev.* **B61**, 2981(2000)

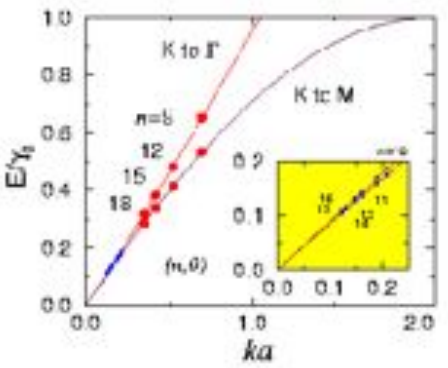

Trigonal warping effect

- 1D Energy Dispersion of SWNT
  - K point is always on a cutting line
  - Two inequivalent neighboring cutting lines --- cause splitting in the density of states

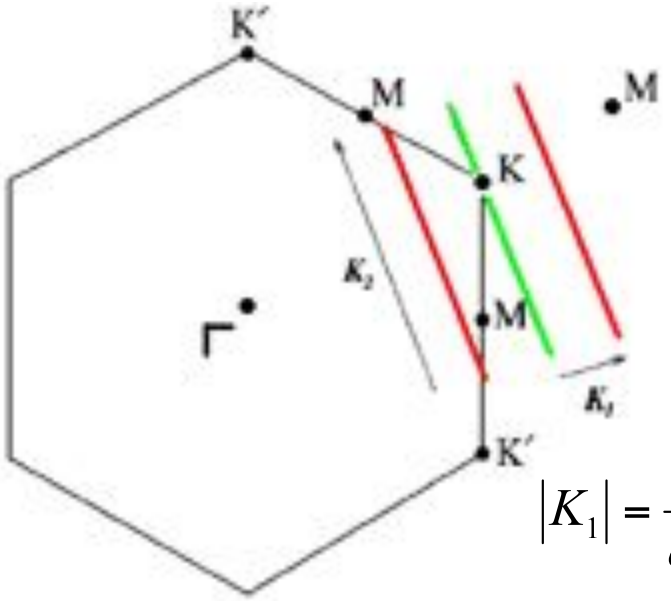

$$|K_1| = \frac{2}{d_t}$$

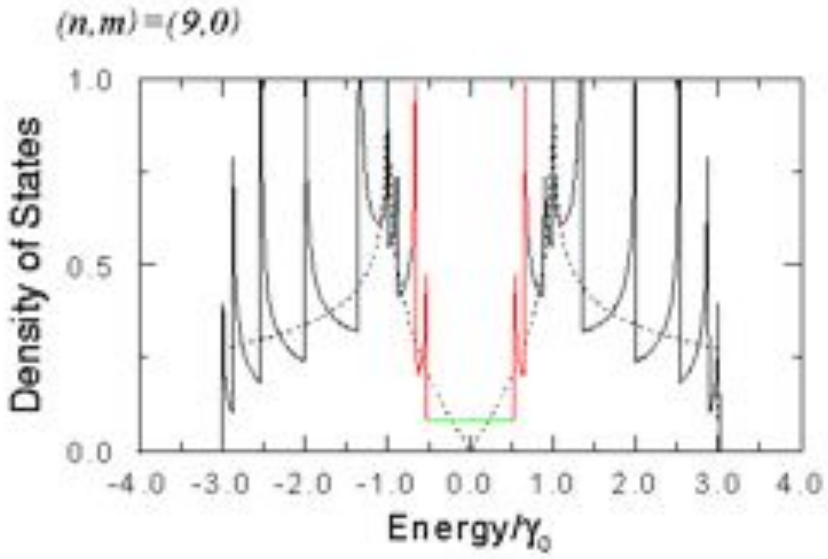

Semiconducting Carbon Nanotubes

R. Saito *et al, Phys. Rev.* **B61**, 2981(2000)

- K points are always at 1/3 (or 2/3) position
  - Two neighboring lines contribute to different energies
  - No DOS splitting for any chirality

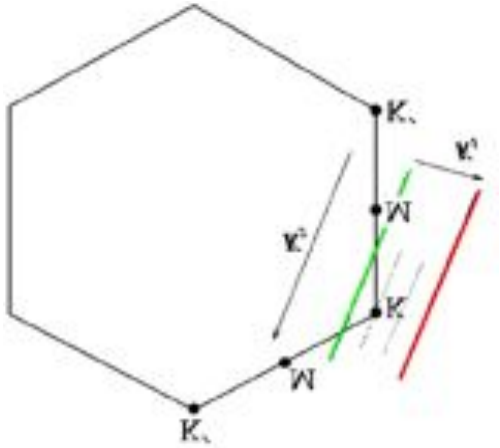

DOS(10,0)

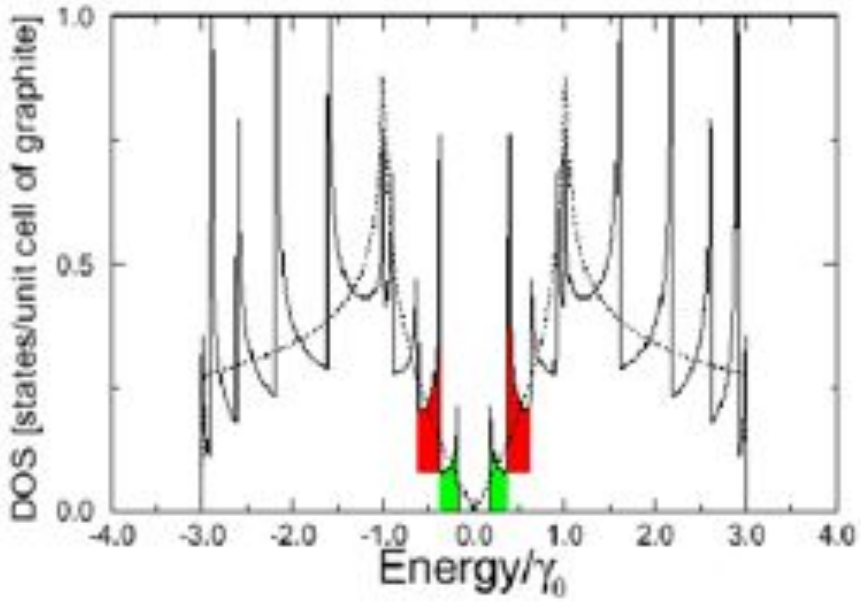

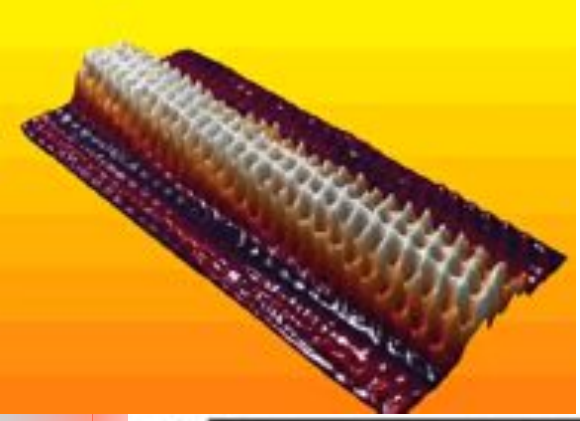

STM/STS

Experiments

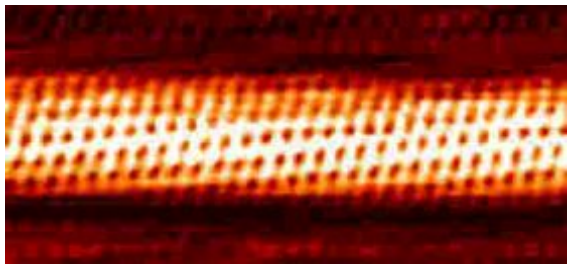

Identified metallic and semiconducting nanotubes

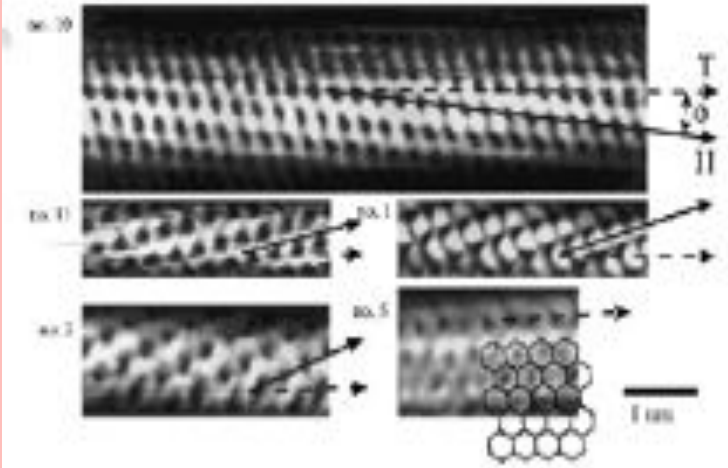

P. Kim et al., PRL 82, (1999) 1225.

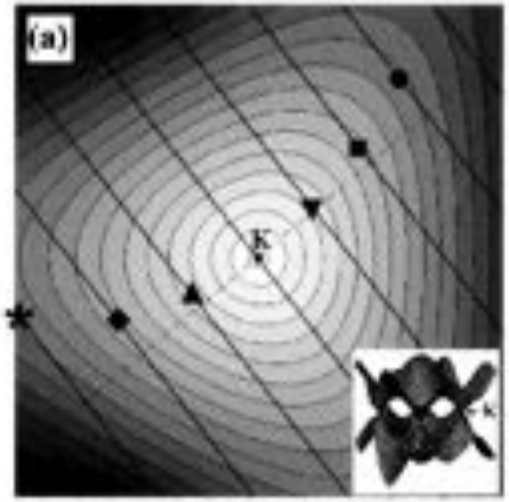

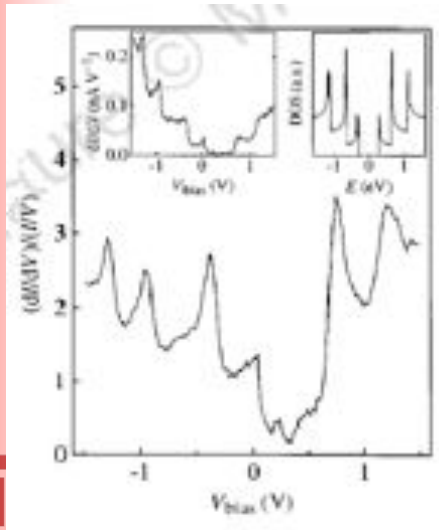

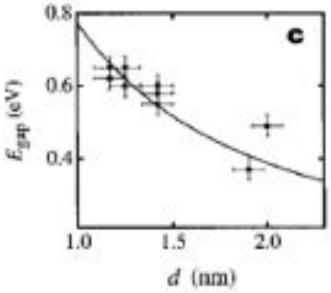

J. W. G. Wildoer et al, Nature, 391 (1998) 59

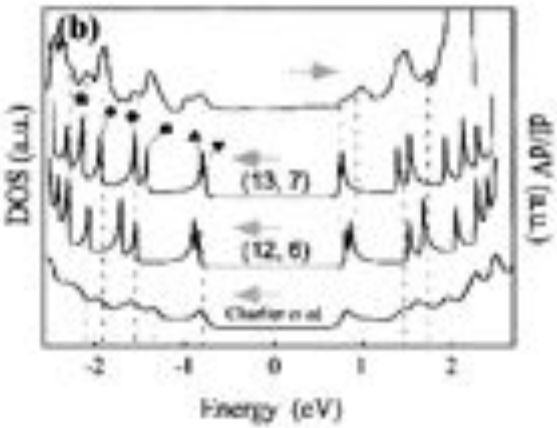

Each (n,m) SWNT has a unique electronic structure

Resonance Raman Spectroscopy (RRS)

A.M. Rao *et al.*, *Science* **275** (1997) 187

RRS: R.C.C. Leite & S.P.S. Porto, PRL **17**, 10-12 (1966)

- Enhanced Signal
  - ✓ Optical Absorption
  - ✓ e-DOS peaks

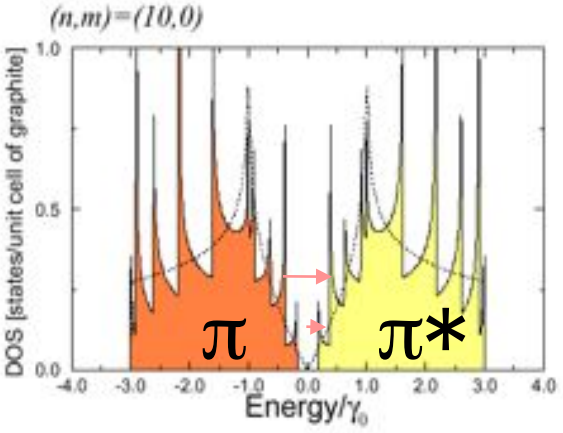

diameter-selective resonance process

$$\omega_{RBM} = \alpha / d_t$$

Confirms:
- Resonant DOS
- Each (*n*,*m*) tube has different spectrum

Raman spectra from SWNT bundles

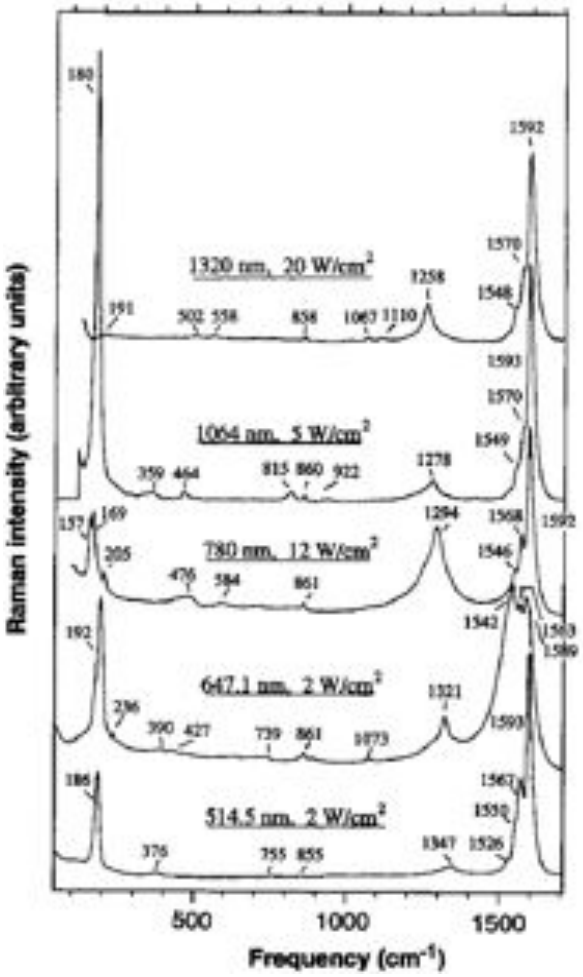

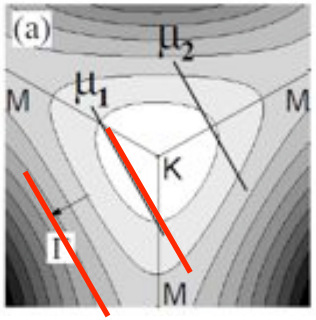

Trigonal warping effect

$E = 0.94\text{eV}$

$= 1.17\text{eV}$

$= 1.58\text{eV}$

$= 1.92\text{eV}$

$= 2.41\text{eV}$

Resonant Raman Spectra of Carbon Nanotube Bundles

M. A. **Pimenta** (UFMG) *et al.*, *Phys. Rev.* B **58**, R16016 (1998)

Metallic and semiconducting tubes have different lineshapes

G-band resonant Raman spectra

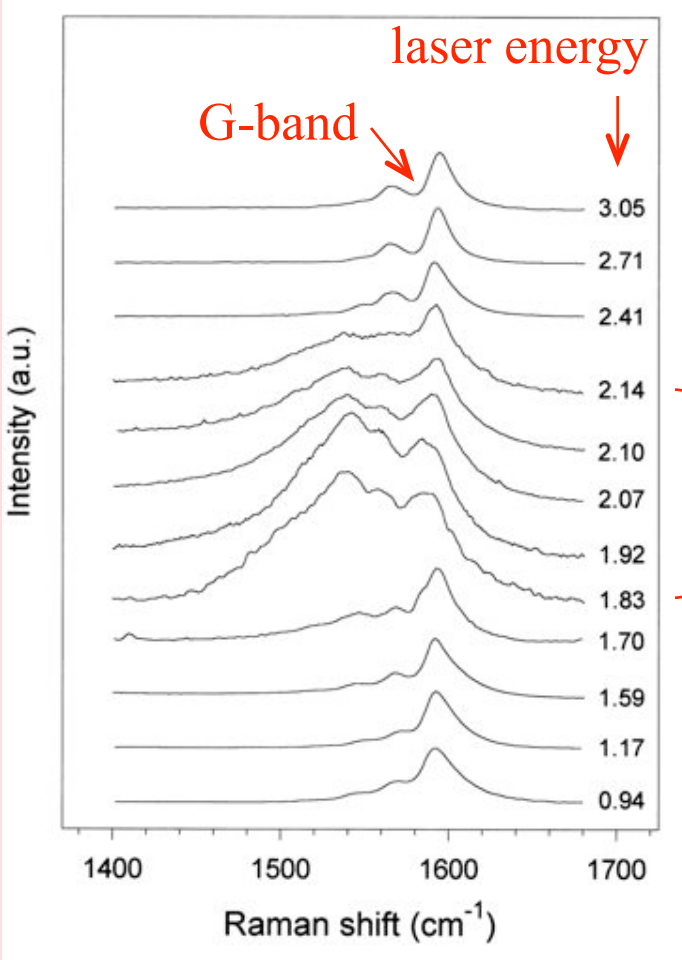

$d_t = 1.37 \pm 0.18$ nm

Diameter dependence of the Van-Hove singularities

Kataura plot

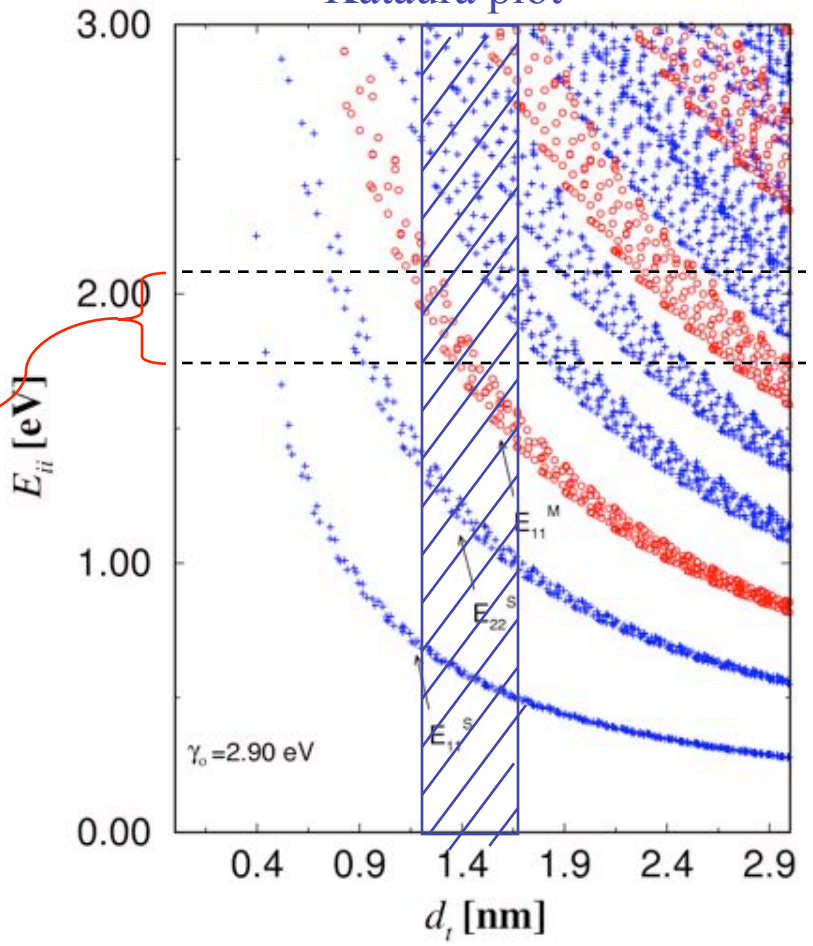

Single Nanotube Spectroscopy yields E_{ii}, (n,m)

Therefore the geometrical structure of an individual carbon nanotube can be found by Raman spectroscopy

A. Jorio (UFMG) ***et al., Phys. Rev. Lett. 86, 1118 (2001)***

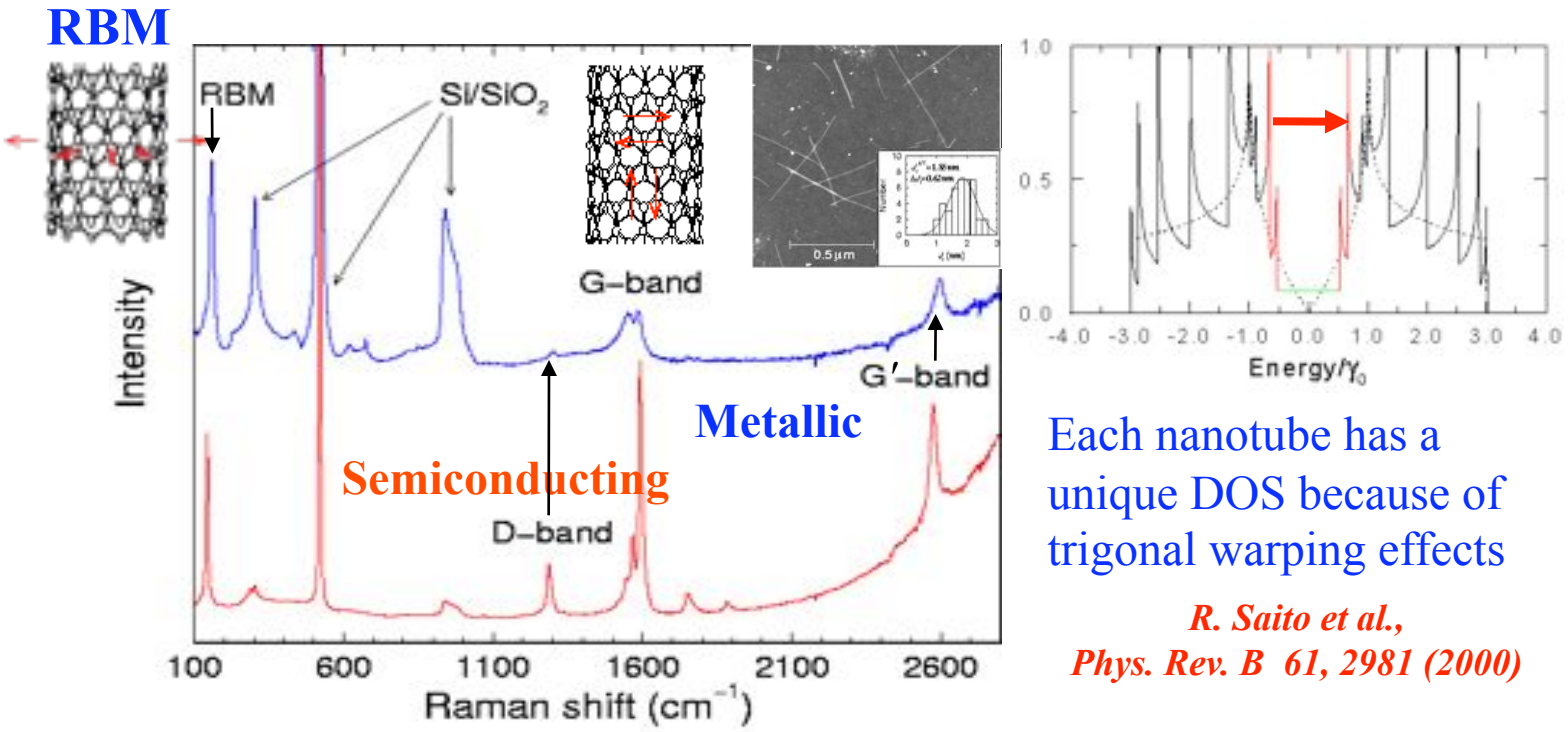

Each nanotube has a unique DOS because of trigonal warping effects

R. Saito et al., Phys. Rev. B 61, 2981 (2000)

Raman signal from *one* SWNT indicates a strong resonance process

$(\omega_{RBM}, E_{ii}) \rightarrow (n,m)$

Raman Spectra of SWNT Bundles

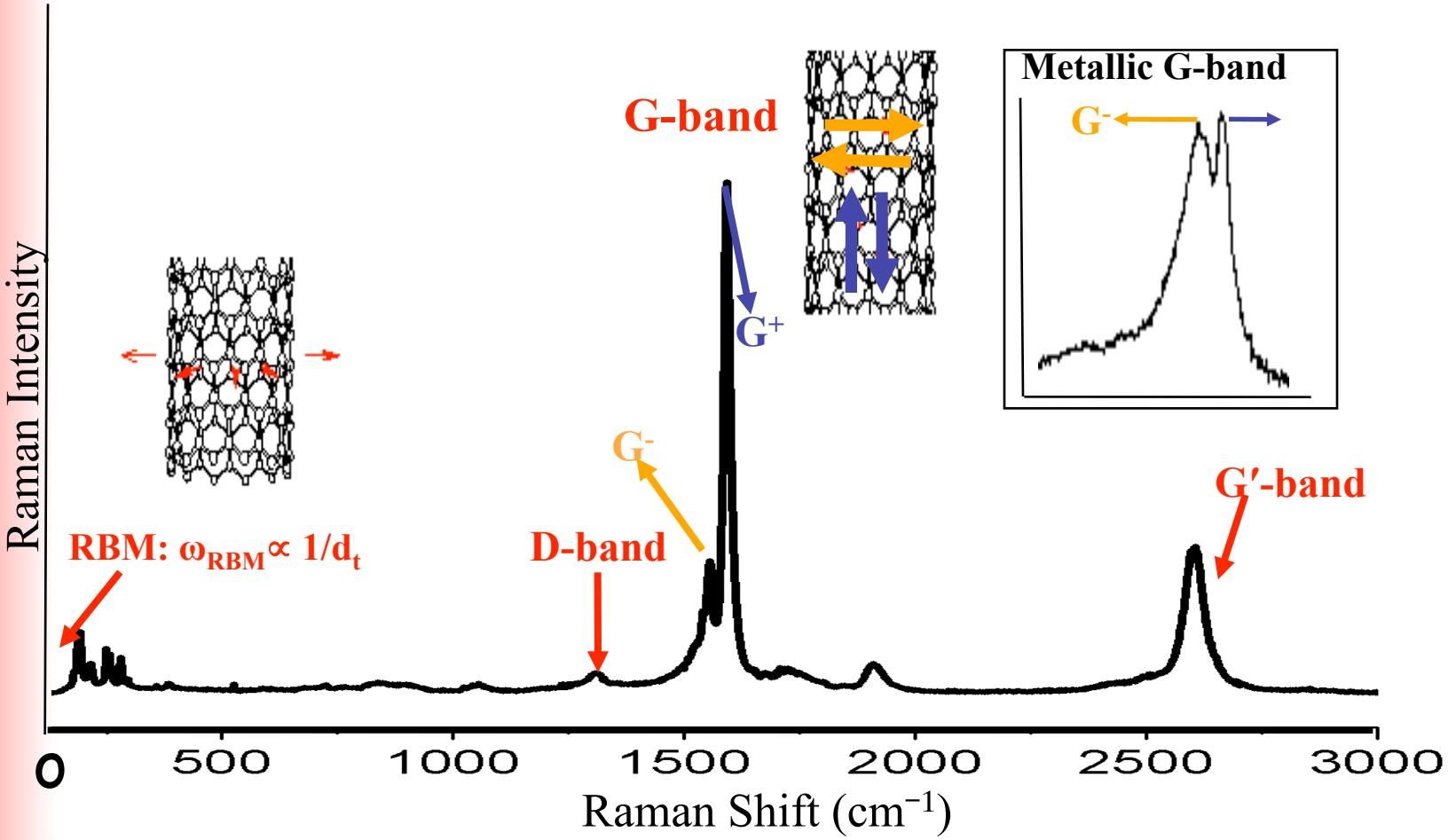

- RBM gives tube diameter and diameter distribution
- Raman D-band characterizes structural disorder
- G^- band distinguished M, S tubes and G^+ relates to charge transfer
- G′ band (2nd order of D-band) provides connection of phonon to its wave vector
- Each feature in the Raman spectra provides complementary information about nanotubes

Band Gap Fluorescence

M. J. O'Connell et al., Science 297 (2002) 593
S. M. Bachilo et al., Science 298 (2002) 2361.

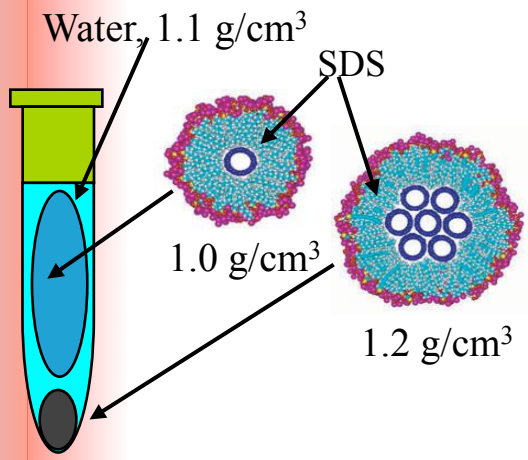

SDS=Sodium Dodecyl Sulfate

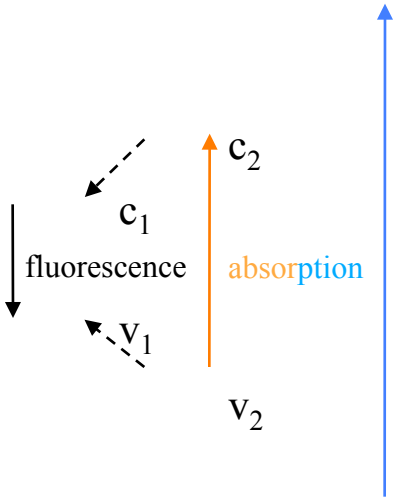

e-DOS of (n, m) = (10,5)

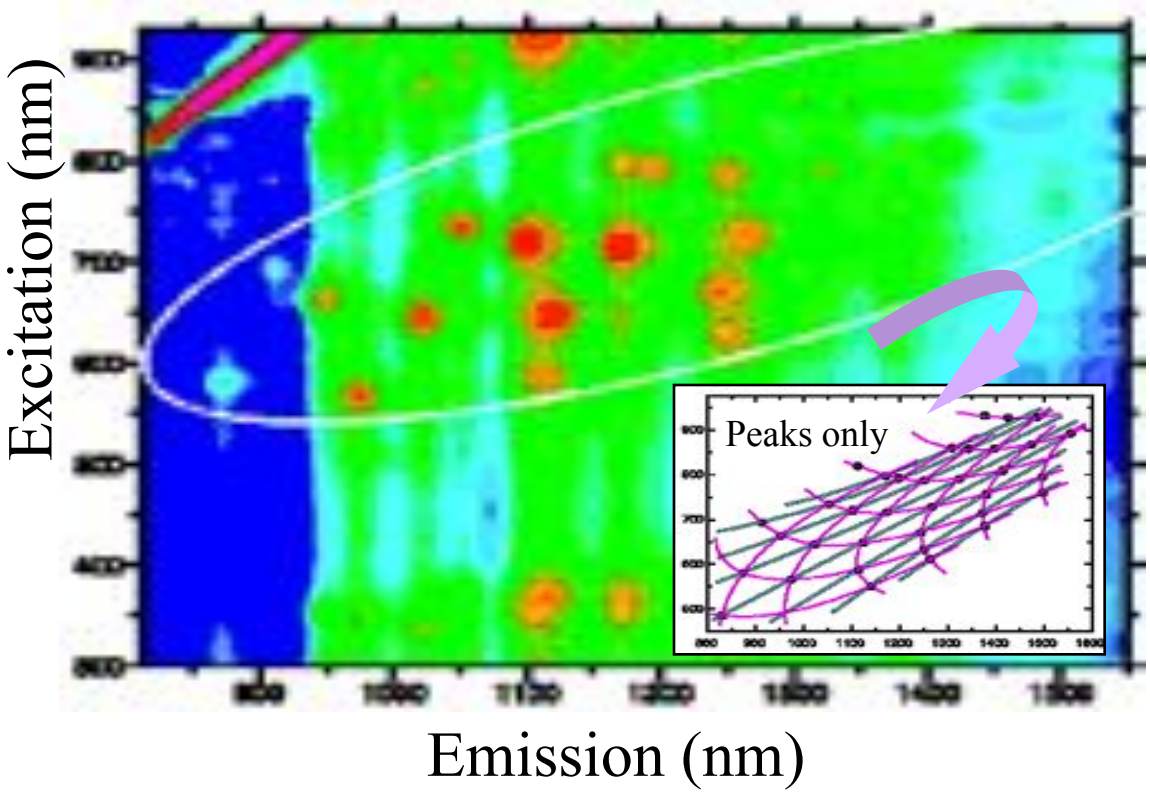

Good method to determine the (n,m) of semiconducting nanotubes in a given sample

Excitons in Carbon Nanotubes

Experimental Justification for excitons

2-photon excitation to a $2A^+$ symmetry exciton (2p) and 1-photon emission from a $1A^-$ exciton (1s) cannot be explained by the free electron model

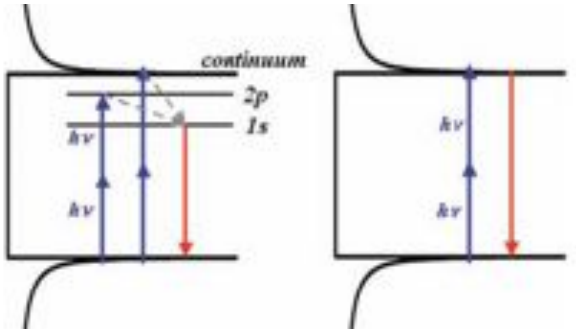

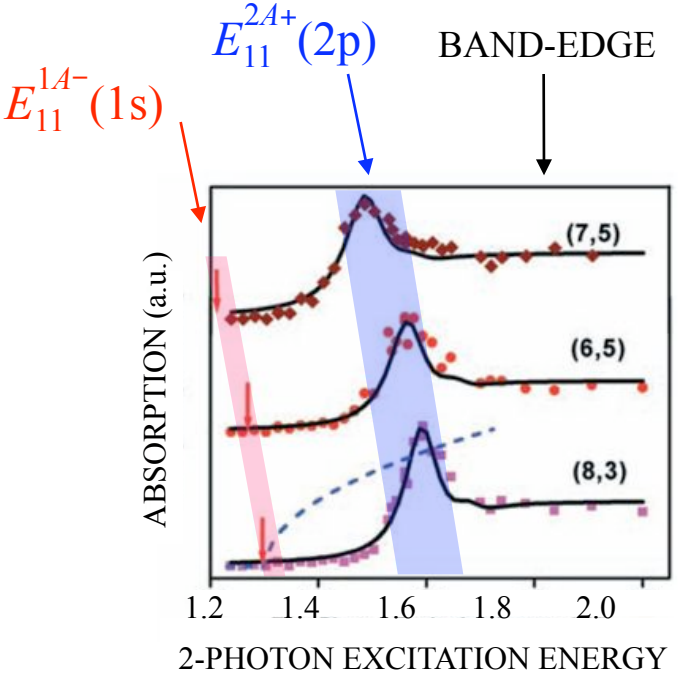

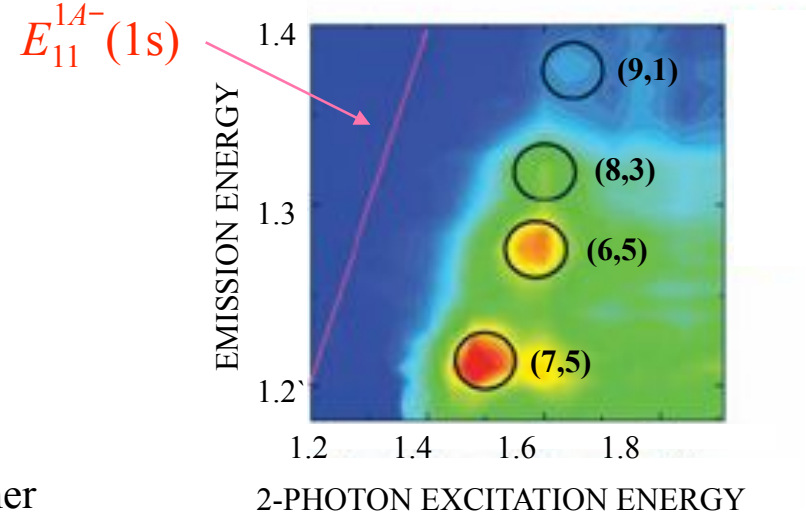

The observation that excitation and emission are at different frequencies supports exciton model rather than free electron model

Wang et al. Science **308**, 838 (2005)

Outline

- Historical Graphene to Graphene path
- Carbon Nanotubes as Prototype Materials
- Disordered Graphite
- Graphene and Graphene Ribbons
- Looking to the Future of Carbon Nanostructures

Raman spectra of graphitic materials: defect detection.

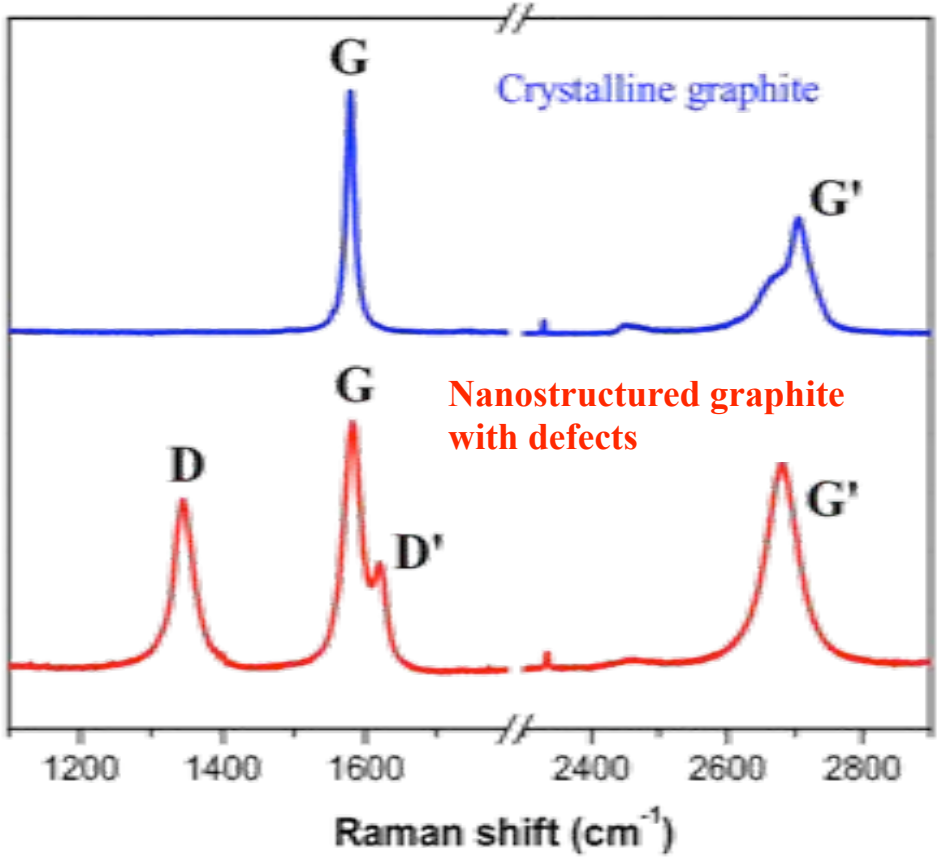

G band:

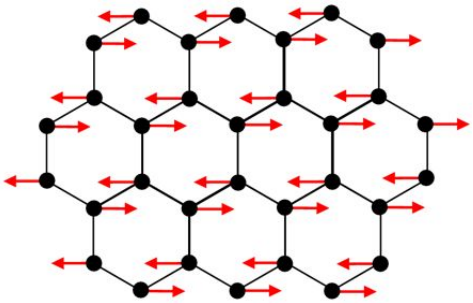

Defect-induced D band:

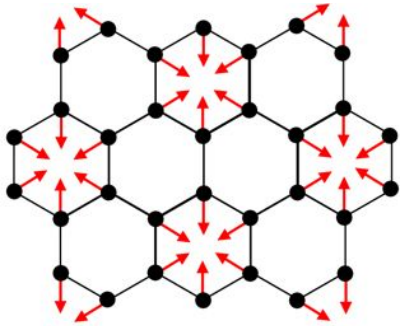

(iTO mode at the K point)

Tuinstra and Koenig, J. Chem. Phys. **53**, 1126 (1970).

Nemanich and Solin, Solid State Comm. **23**, 417 (1977).

Tsu *et al.*, Solid State Commun. **27**, 507 (1978).

G′ band: Second harmonic of D band.

(also called 2D band)

Intravalley double-resonance process Explains the D′ band process

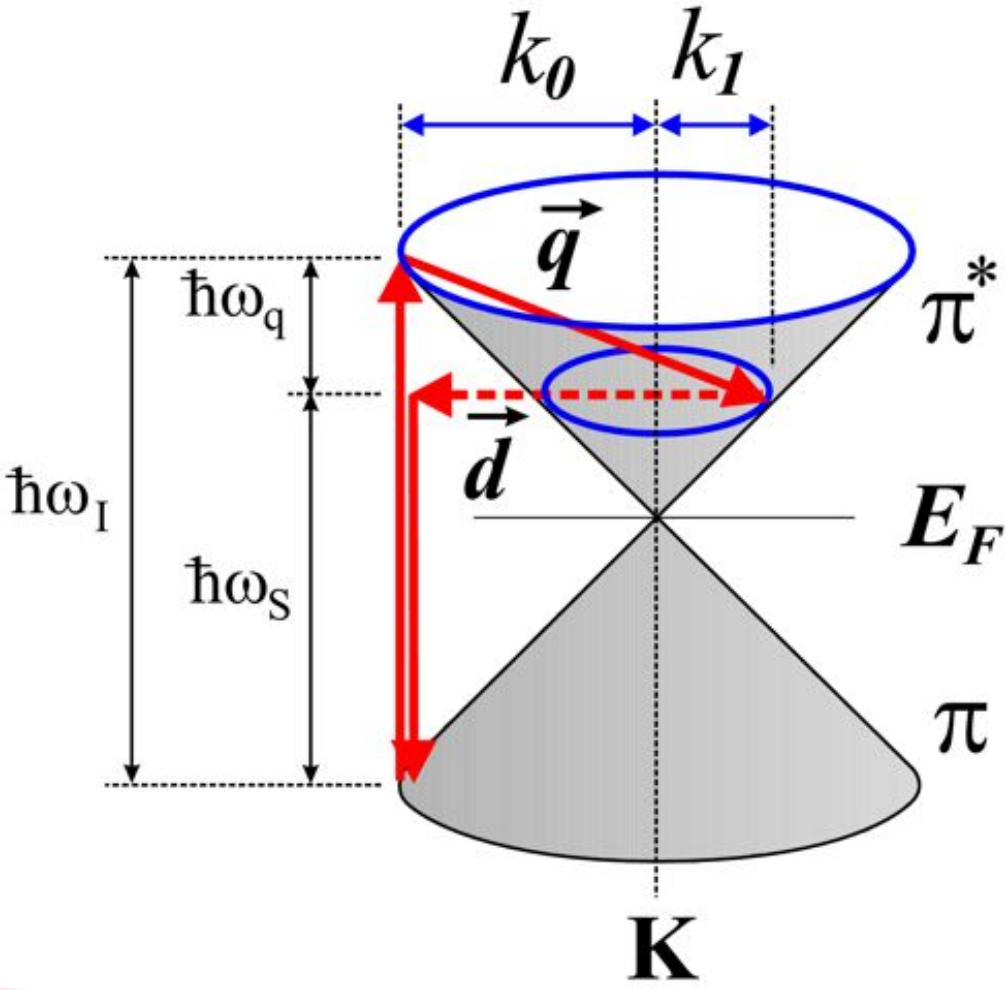

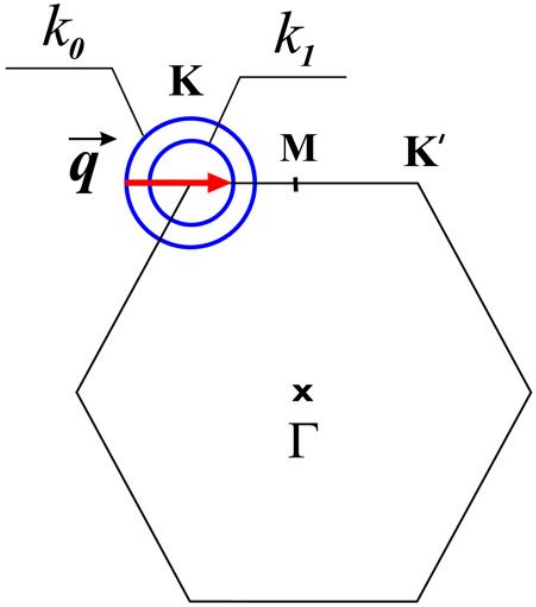

$$k_0 = \hbar\omega_I / 2v_F$$

$$k_1 = k_0 - \hbar\omega_q / v_F$$

Baranov *et al.*, Opt. Spectrosc. USSR **62**, 612 (1987).
Thomsen and Reich, Phys. Rev. Lett. **85**, 5214 (2000).

Intervalley double-resonance process

Explains the origin of the D-band

Scattering by defect in an energy conserving process

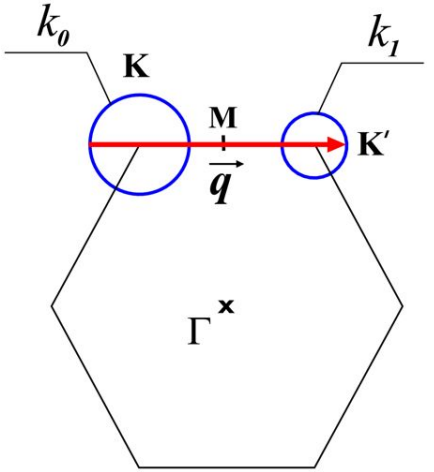

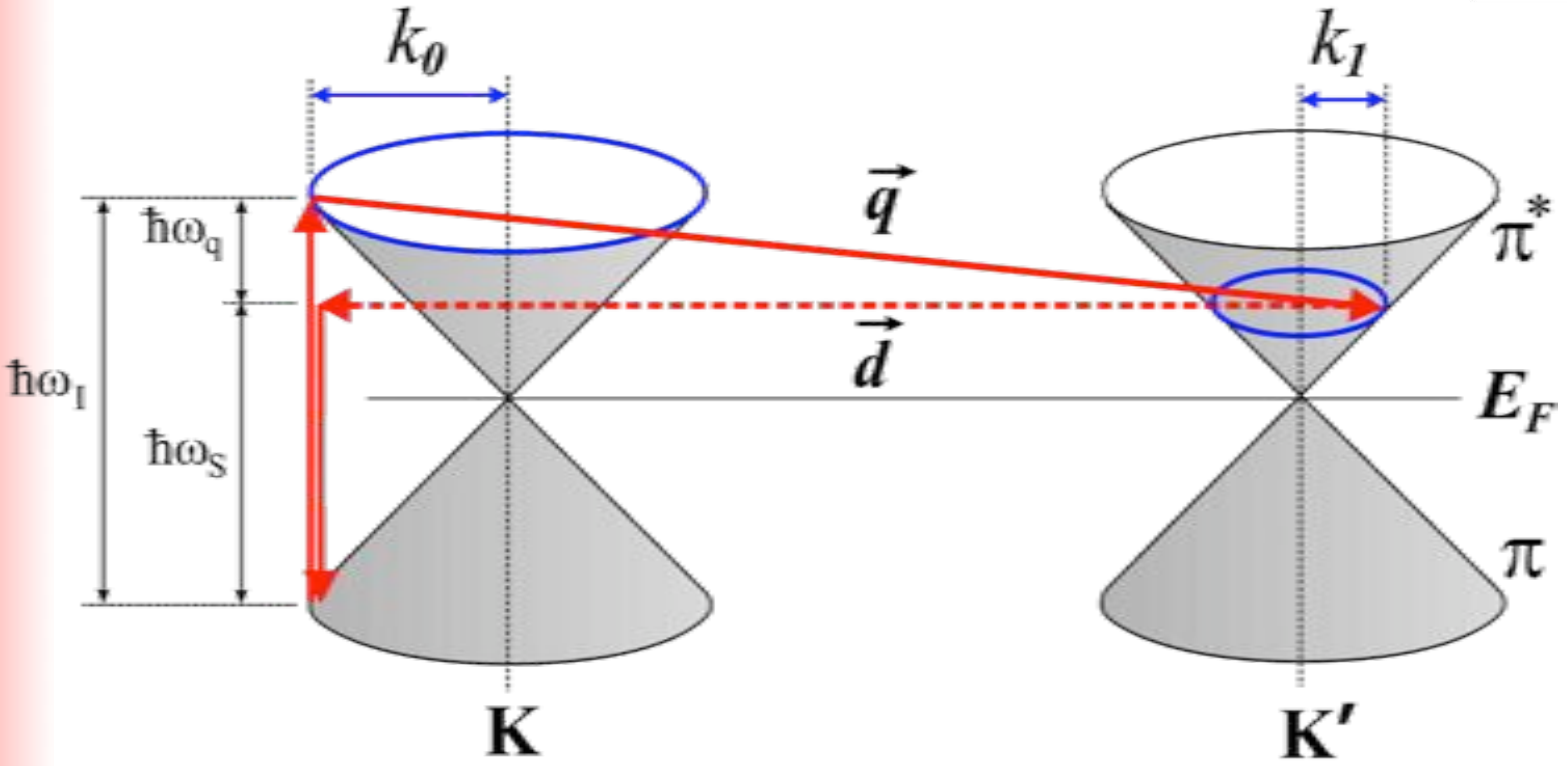

Saito *et al.*, Phys. Rev. Lett. **88**, 027401 (2002).

Intravalley *vs.* intervalley double-resonance processes

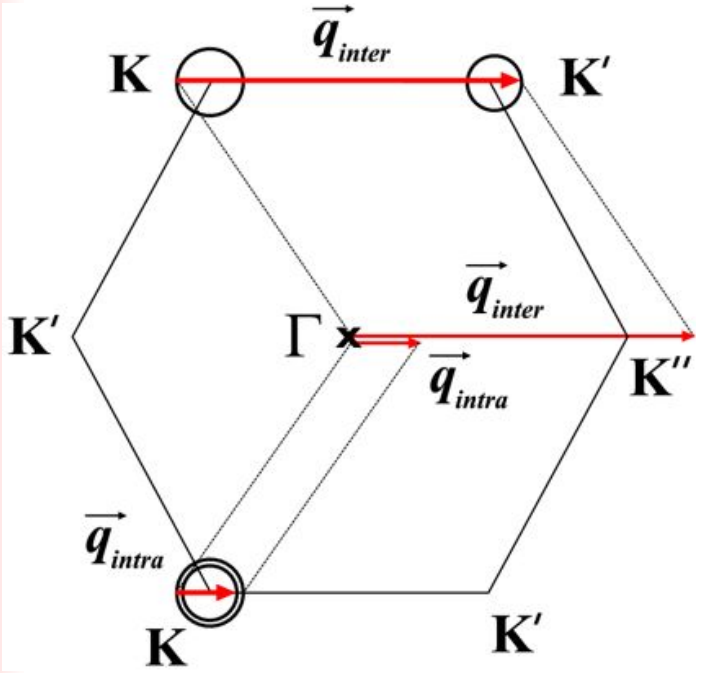

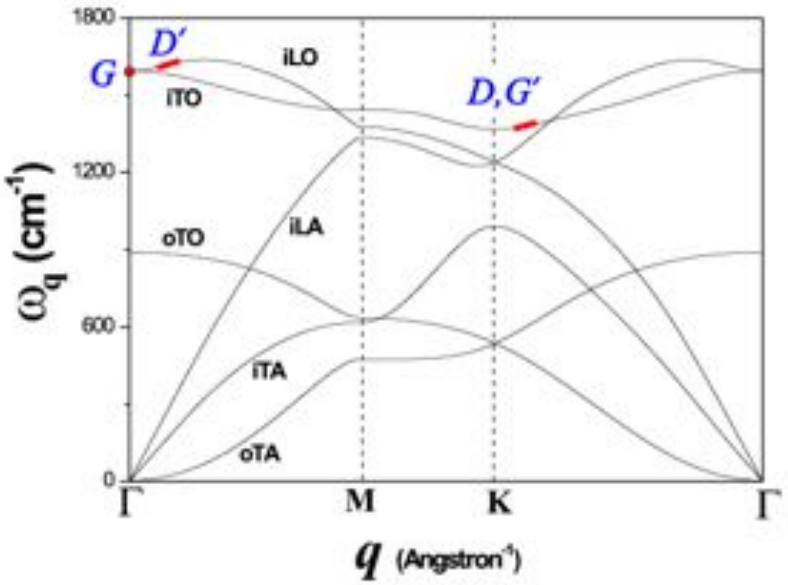

Saito *et al.*, Phys. Rev. Lett. **88**, 027401 (2002).

G band: first order allowed (closed to the Γ point).
D′ band: double resonance intravalley process.
D and G′ bands: double resonance intervalley process.

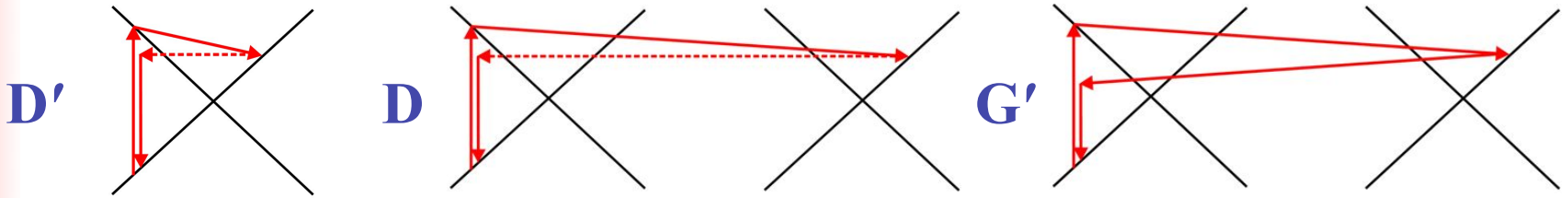

Determination of the average crystallite size L_a of nanographite films by STM and X-ray diffraction using sychrotron radiation

The values of L_a obtained by STM and X-ray diffraction are in good agreement:

HTT (°C)	L_a (nm) (X ray)	L_a (nm) (STM)
2700	490	550
2600	340	300
2400	190	220
2300	150	120
2200	65	60
2000	35	40
1800	20	20

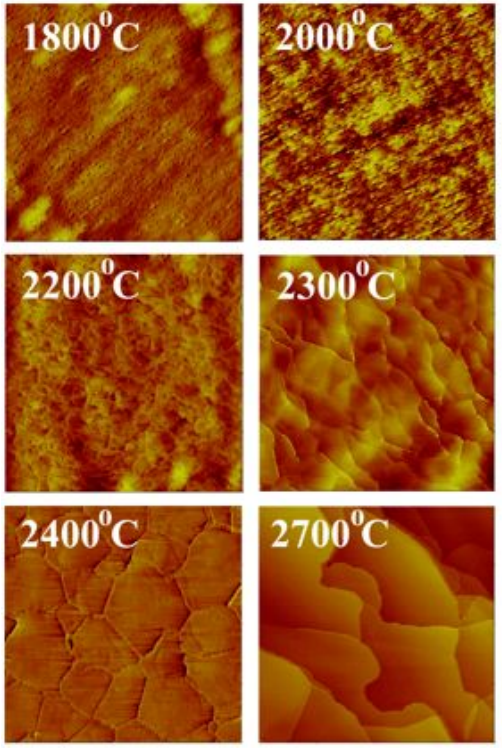

(a)

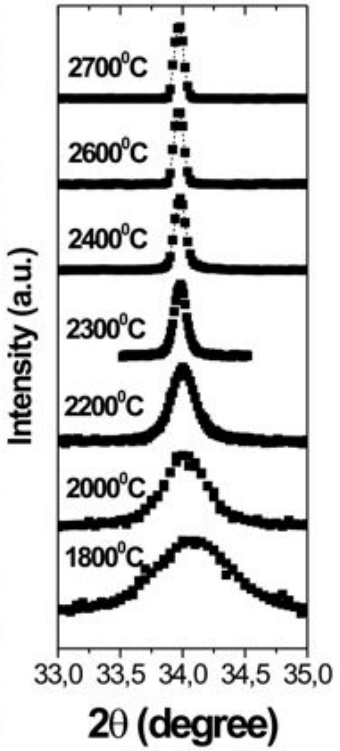

(b)

The same samples are used for Raman characterization of L_a

Cançado *et al.*, App. Phys. Lett. **88**, 163106 (2006).

Dependence of the ratio I_D / I_G on the crystallite size L_a in the Raman spectra of disordered graphite

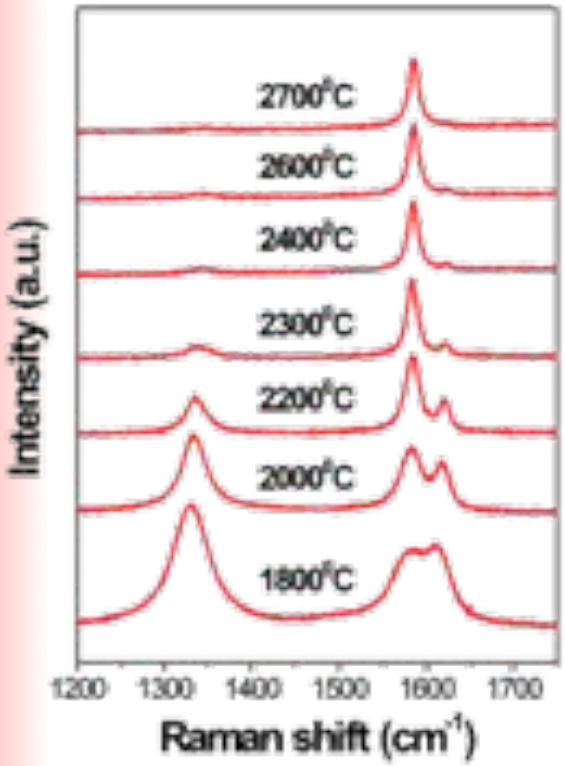

Cançado *et al.*, App. Phys. Lett. **88**, 163106 (2006).

$$L_a = \kappa \left[\frac{I_D}{I_G}\right]^{-1}$$

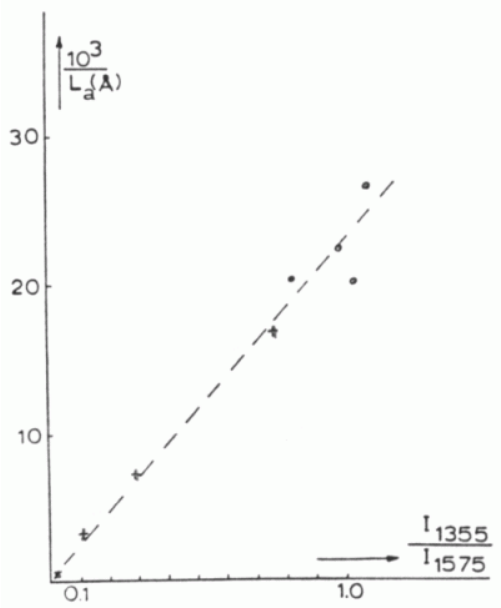

Tuinstra and Koenig, *J. Chem. Phys.* **53**, 1126 (1970).
Tuinstra and Koenig, *J. Compos. Mater* **4**, 492 (1970).

κ = 4.4nm for λ = 514.5 nm (2.41eV)
Knight and White, J. Mater. Res. **4**, 385 (1989).

Dependence of the ratio I_D / I_G on the excitation laser energy E_l in the Raman spectra of disordered graphite

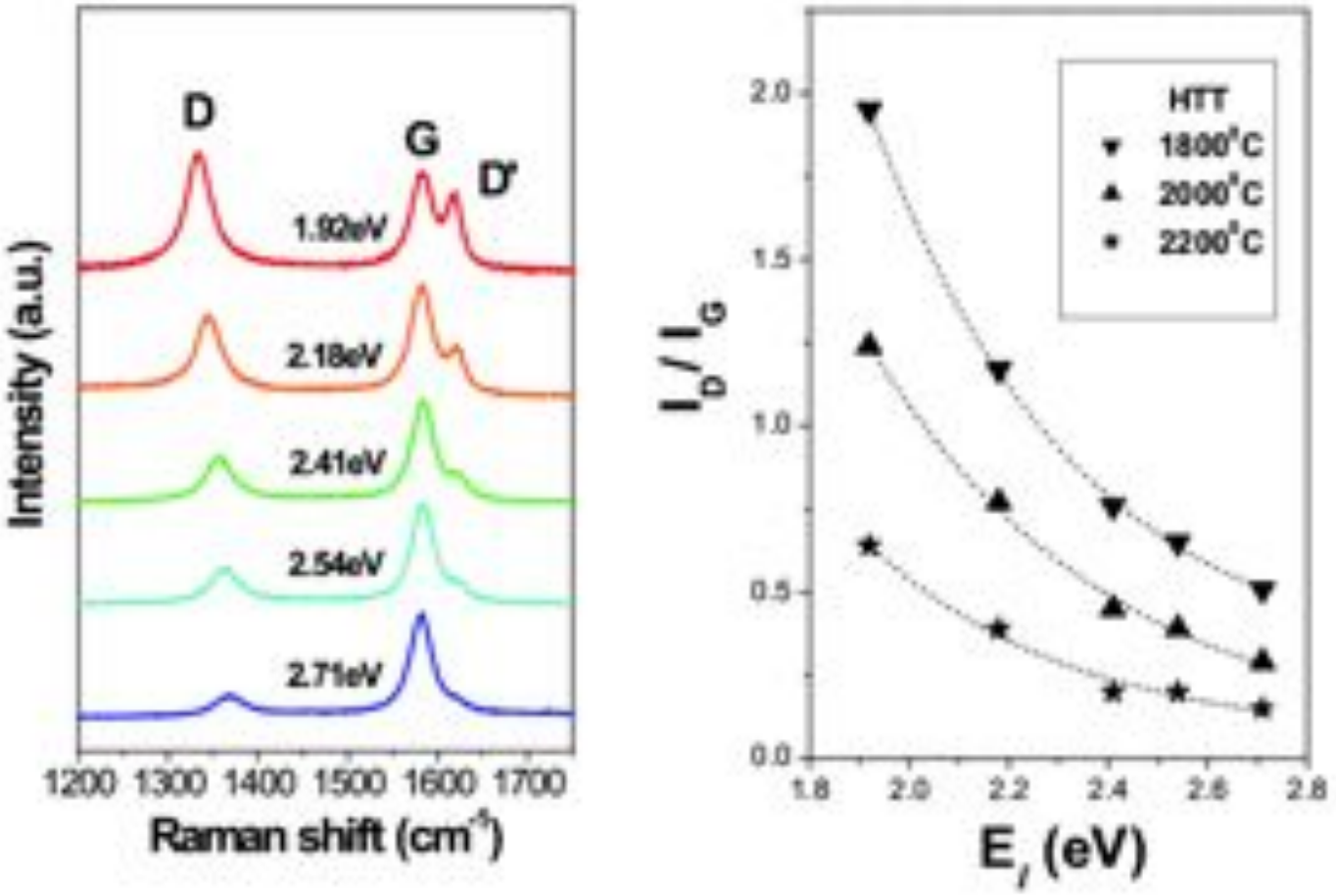

Cançado *et al.*, App. Phys. Lett. **88**, 163106 (2006).

Mernagh *et al.,* Carbon **22**, 39 (1984).

General equation for the determination of the crystallite size L_a of nanographite by Raman spectroscopy

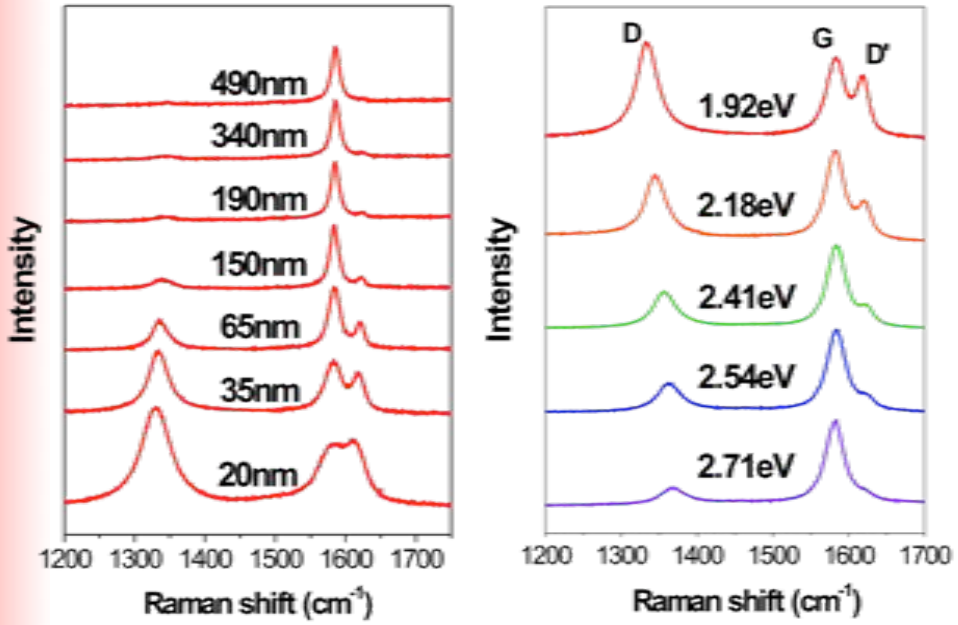

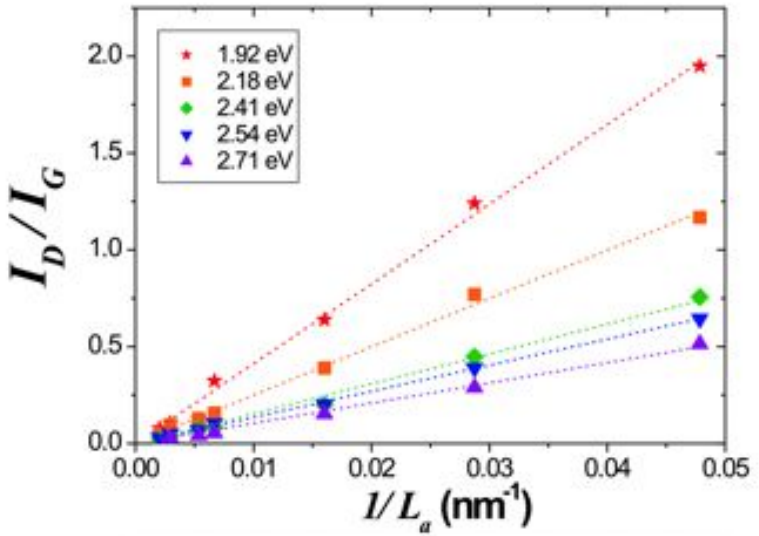

$$L_a(\text{nm}) = \frac{560}{E_l^4}\left(\frac{I_D}{I_G}\right)^{-1}$$

$$L_a(\text{nm}) = (2.4 \times 10^{-10})\lambda_l^4\left(\frac{I_D}{I_G}\right)^{-1}$$

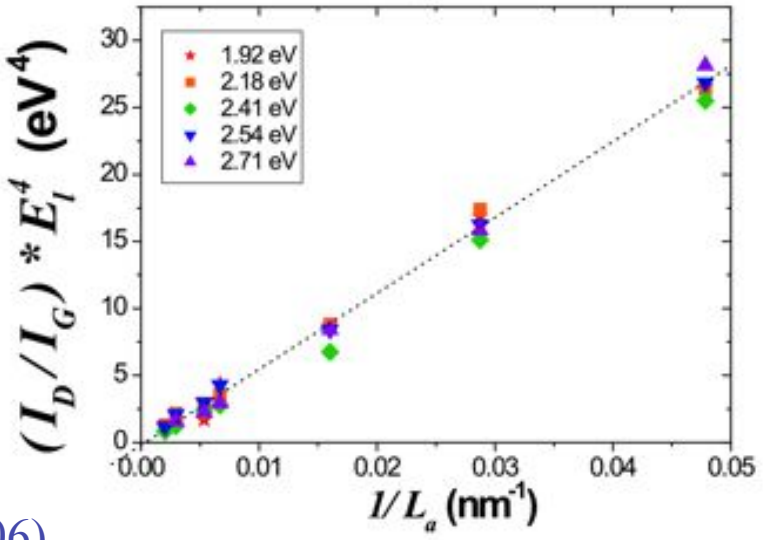

Cançado *et al.*, Appl. Phys. Lett. **88**, 163106 (2006).

Measuring the dependence of the differential cross section of the Raman bands in graphite on the excitation laser energy E_l

Normalized to G-band intensity

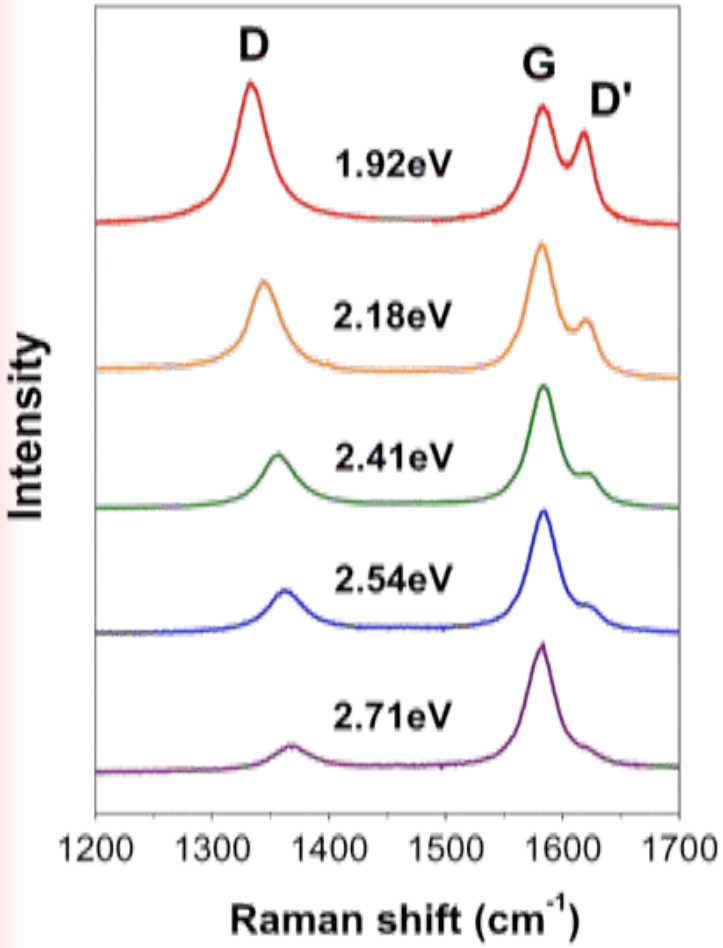

Direct intensity measurement

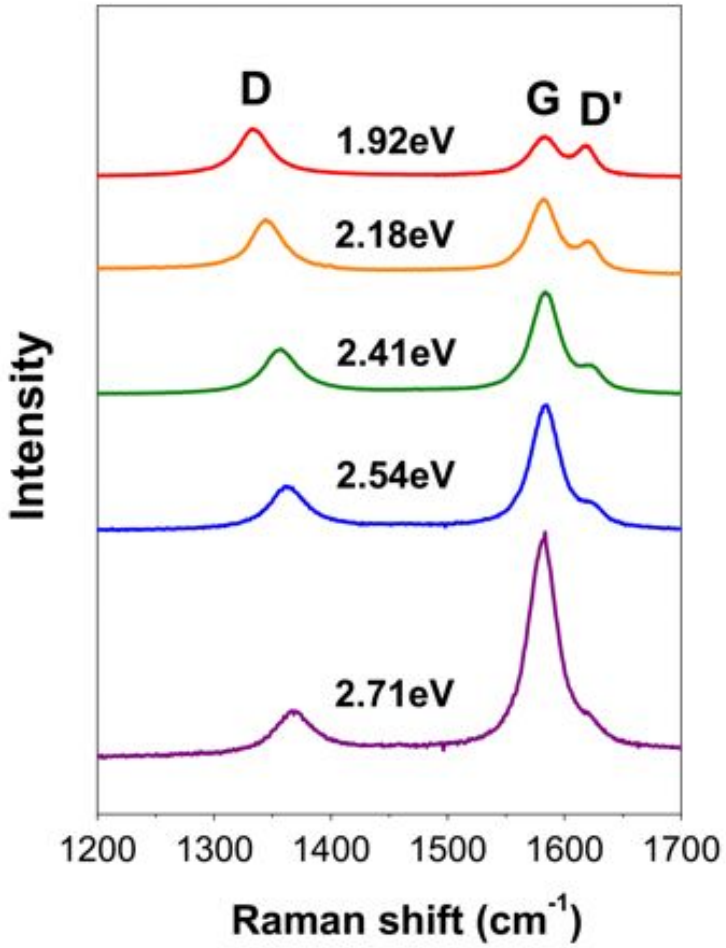

Cançado *et al.*, Phys. Rev. B. **76**, 064304 (2007).

Measuring the dependence of the differential cross section of the Raman bands in graphite on the excitation laser energy E_l

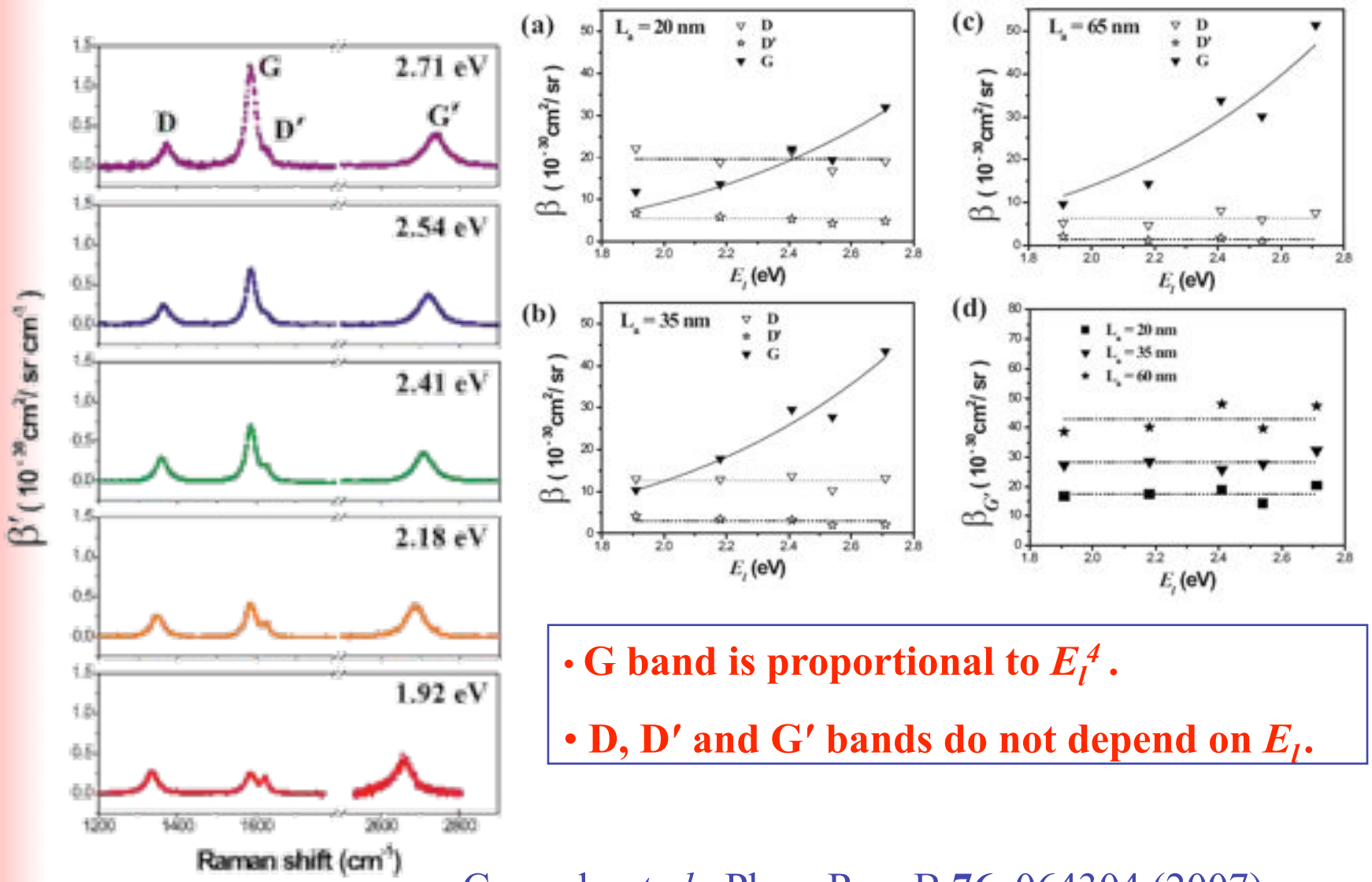

- G band is proportional to E_l^4 .
- D, D′ and G′ bands do not depend on E_l.

Cançado *et al.*, Phys. Rev. B **76**, 064304 (2007).

Quantifying the stacking order in nanographites by Raman spectroscopy

$$R = \left| \frac{I_{G'_{3DB}}}{I_{G'_{3DB}} + I_{G'_{2D}}} \right|$$

$$v_{3D} = R, \text{ and } v_{2D} = 1 - R$$

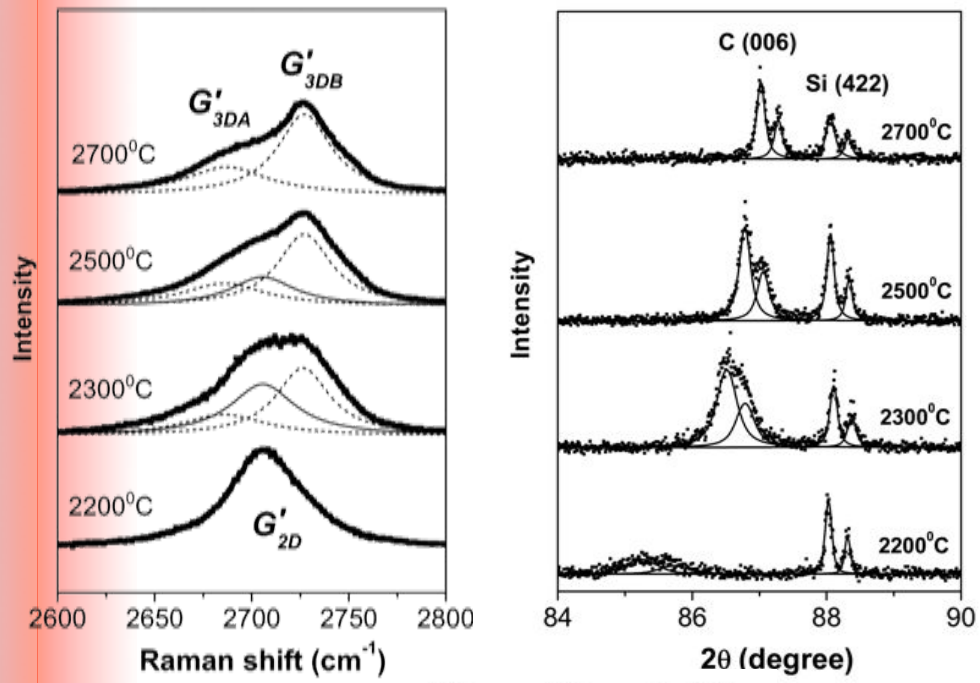

$$V = V_{3D} + V_{2D}$$

$$v_{3D} = V_{3D}/V \text{ and } v_{2D} = V_{2D}/V$$

$$c\,(nm) = 0.682 - 0.11R$$

$$L_c\,(nm) = 10 + \frac{10}{1.05 - R}$$

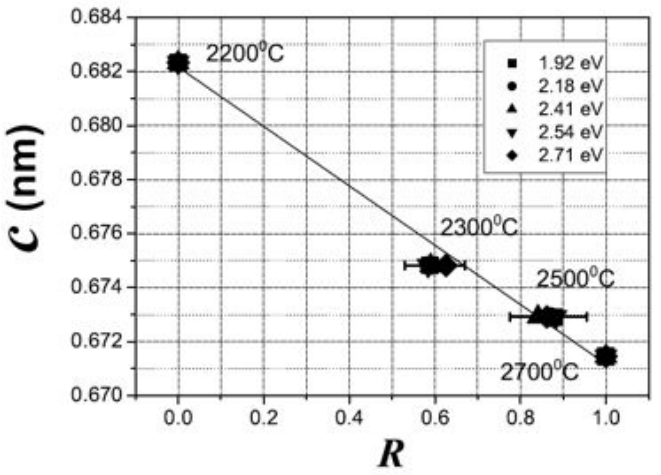

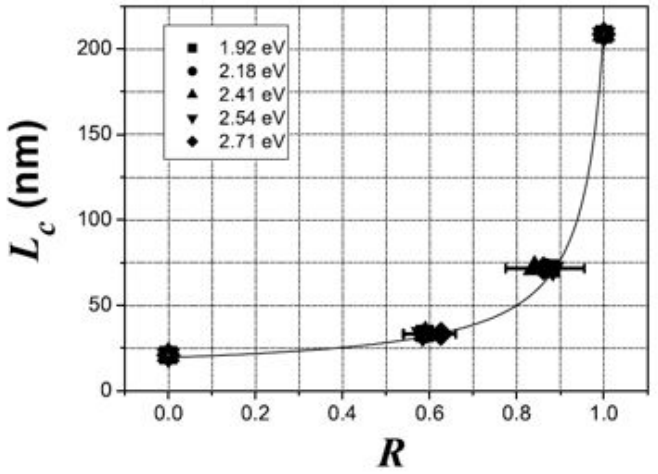

Cançado *et al.*, Carbon **46**, 272 (2008).

Outline

- Historical Graphene to Graphene path
- Carbon Nanotubes as Prototype Materials
- Disordered Graphite
- Graphene and Graphene Ribbons
- Looking to the Future of Carbon Nanostructures

Electronic structures of graphene and bilayer graphene

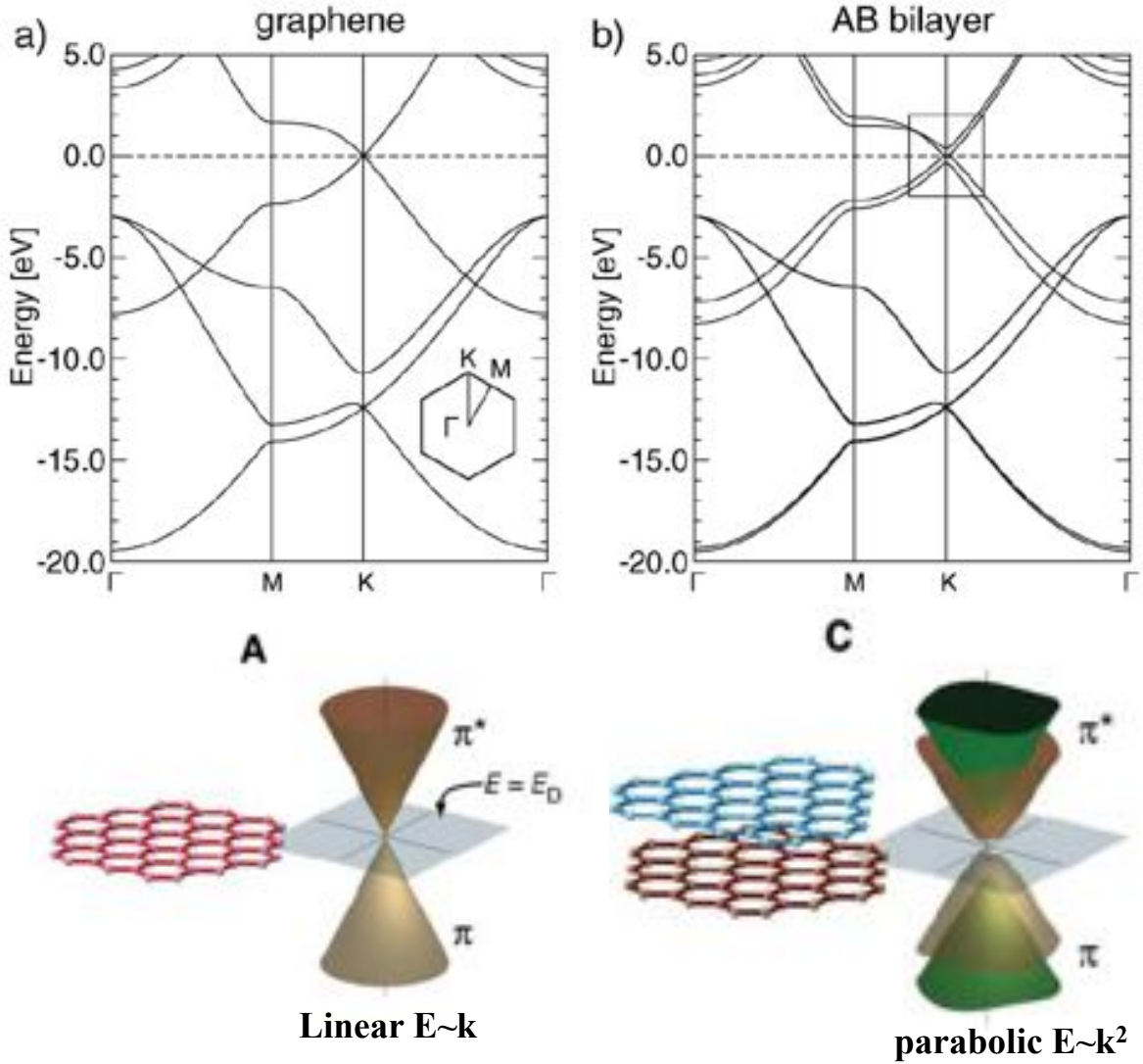

Linear E~k **parabolic E~k²**

Sylvain Latil and Luc Henrard, Phys. Rev. Lett. **97**, 036803 (2006).

Taisuke Ohta, *et al.,* Science **313**, 951 (2006).

Raman G′ band identifies the number of layers

Distinguishes graphite from graphene

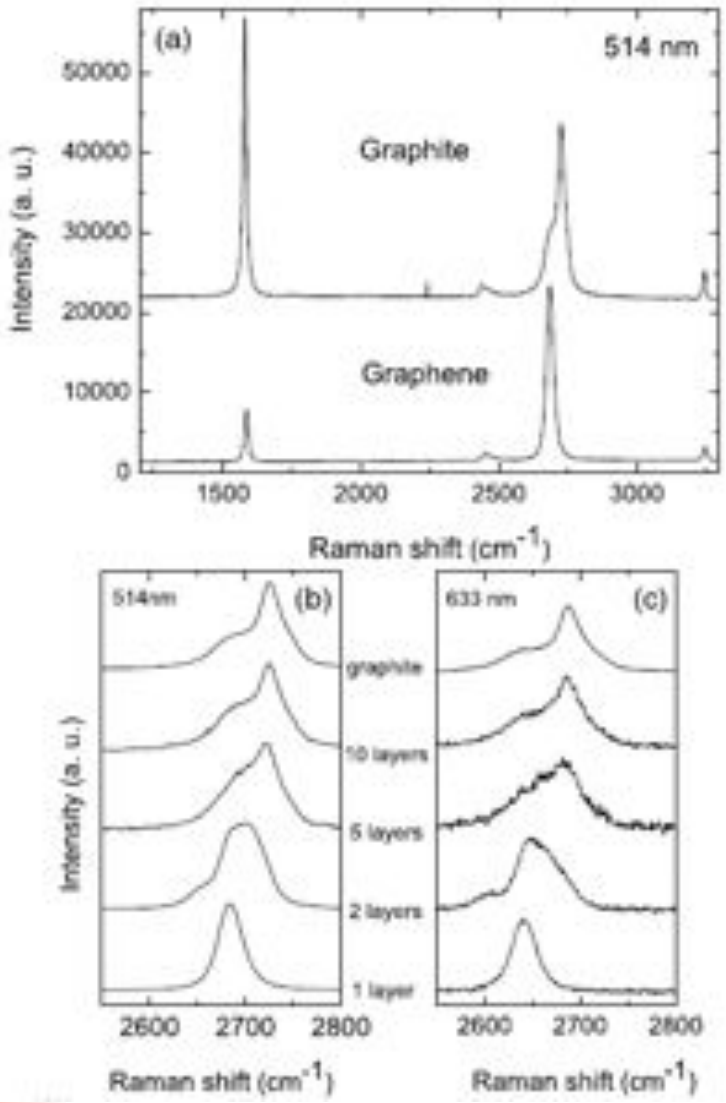

Identifies the number of graphene layers

***G′* (3D graphite) – two peaks**

***G′* (2D graphite) – one peak**

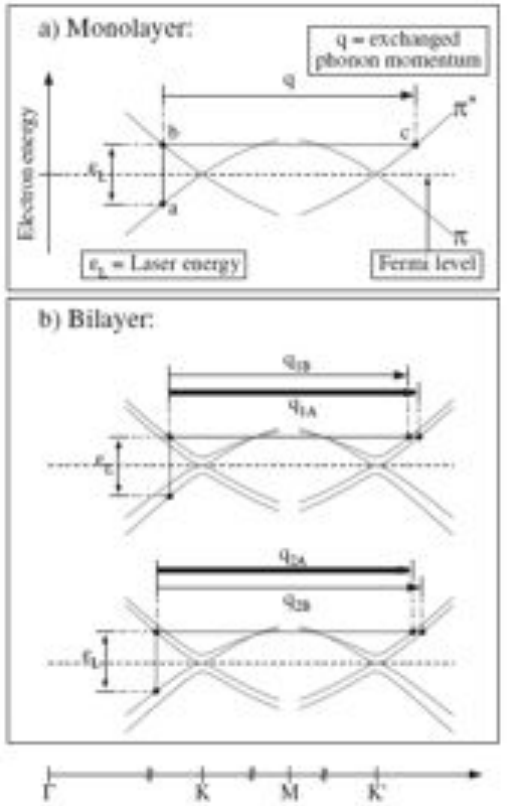

•Ferrari *et al.,* Phys. Rev. Lett. **97,** 187401 (2006).

• Gupta *et al.,* Nanoletters **6**, 2667 (2006).

• Graf *et al.,* Nanoletters, (2007).

Raman confocal image of single graphene layer

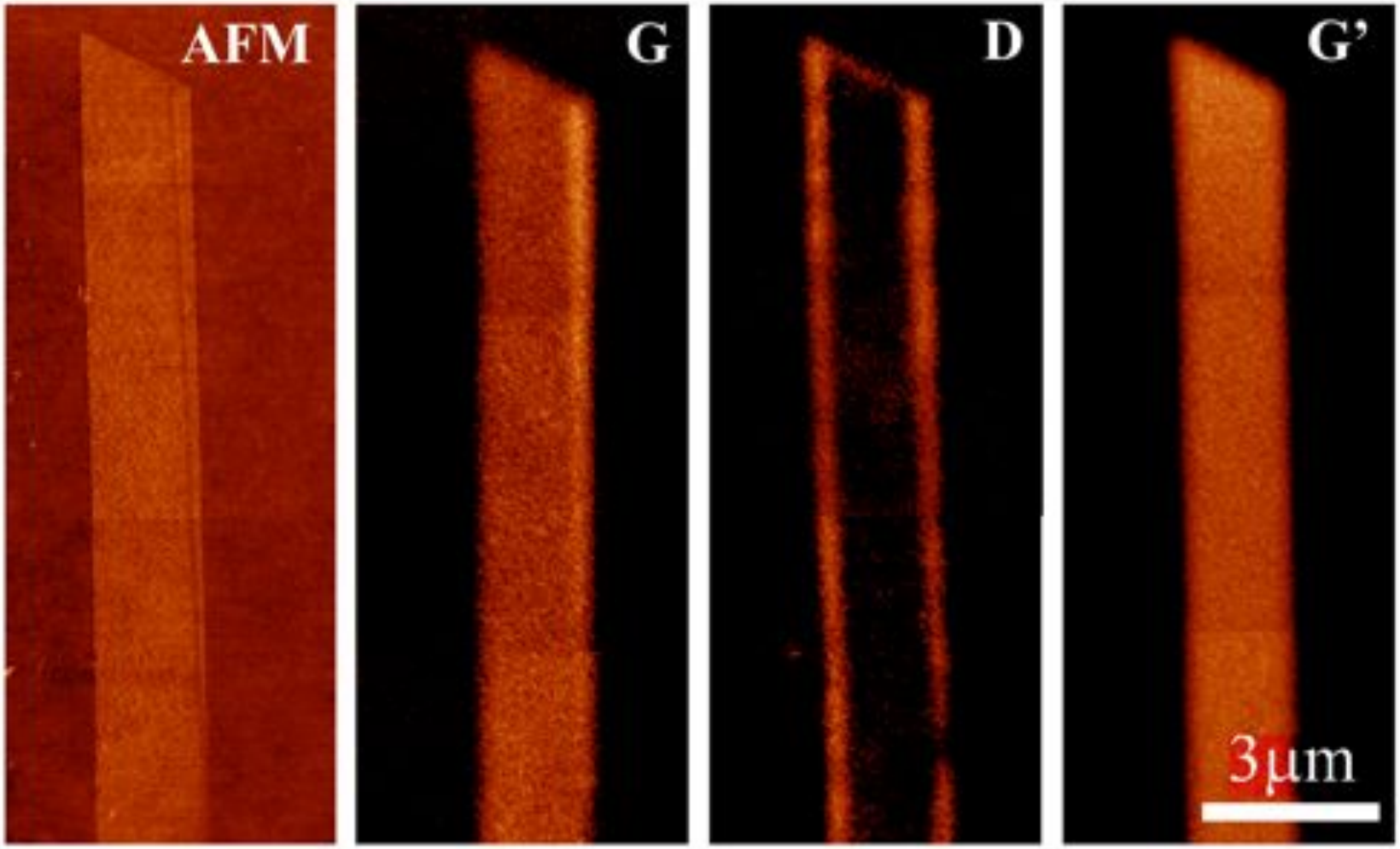

The D band is detected only at the edges in contrast to the G-band and G′-band.

Near-field optics

Conventional microscope

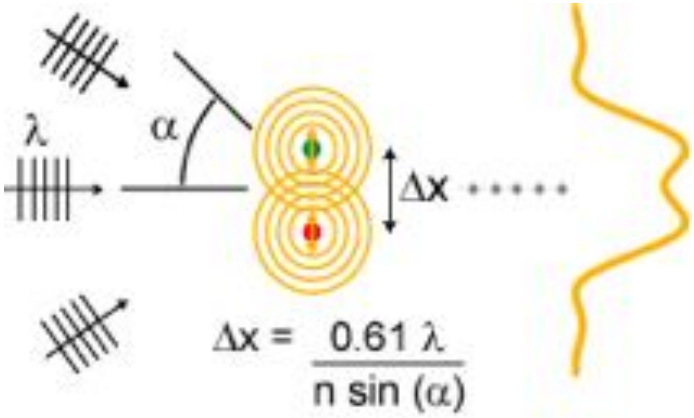

Abbé, Arch. Mikrosk., Anat.,(1873).

Conventional microscopy limited by diffraction effects.

Near-field microscope

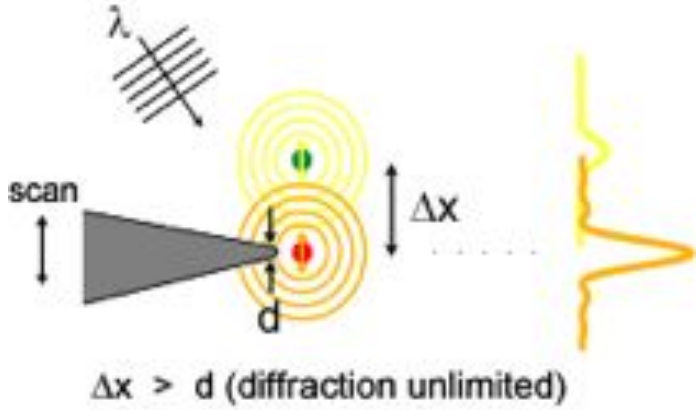

Wessel, JOSA B, (1985).
Novotny et al., Ultramicroscopy, (1998).

Near-field microscopy permits independent interaction between tip and sample.

STRUCTURAL DEFECTS IN BURIED NANOTUBES

Topography:

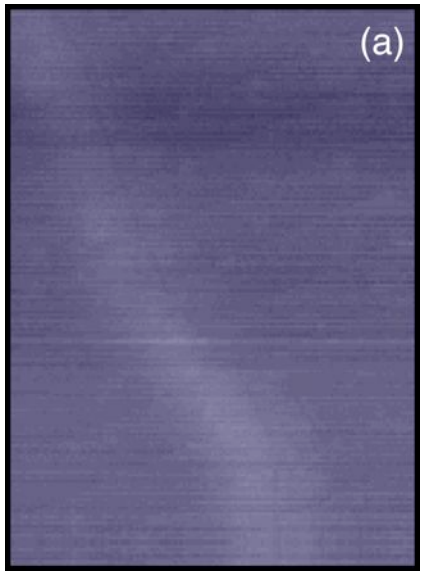

Confocal Raman:

Near-field Raman:

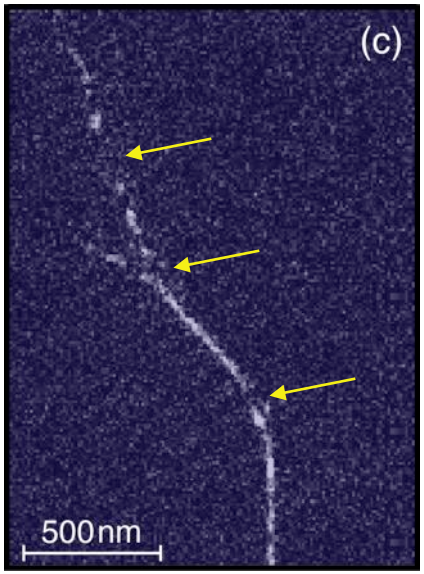

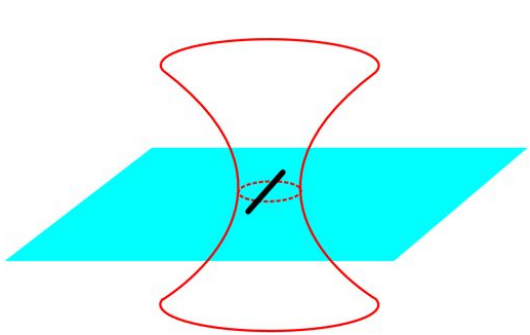

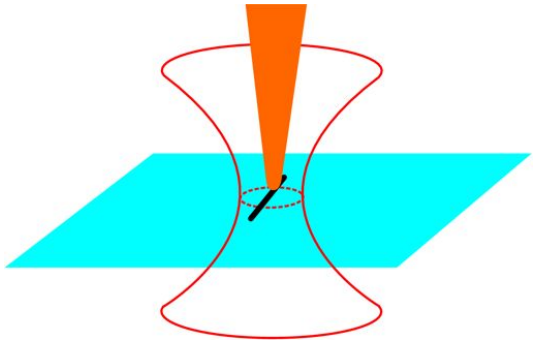

Structural variations (defects, branching, ..) hidden in confocal imaging !

Nano Lett. **6, 744 (2006).**

Out-of-plane modes show larger enhancement than in-plane modes:

In near field optics

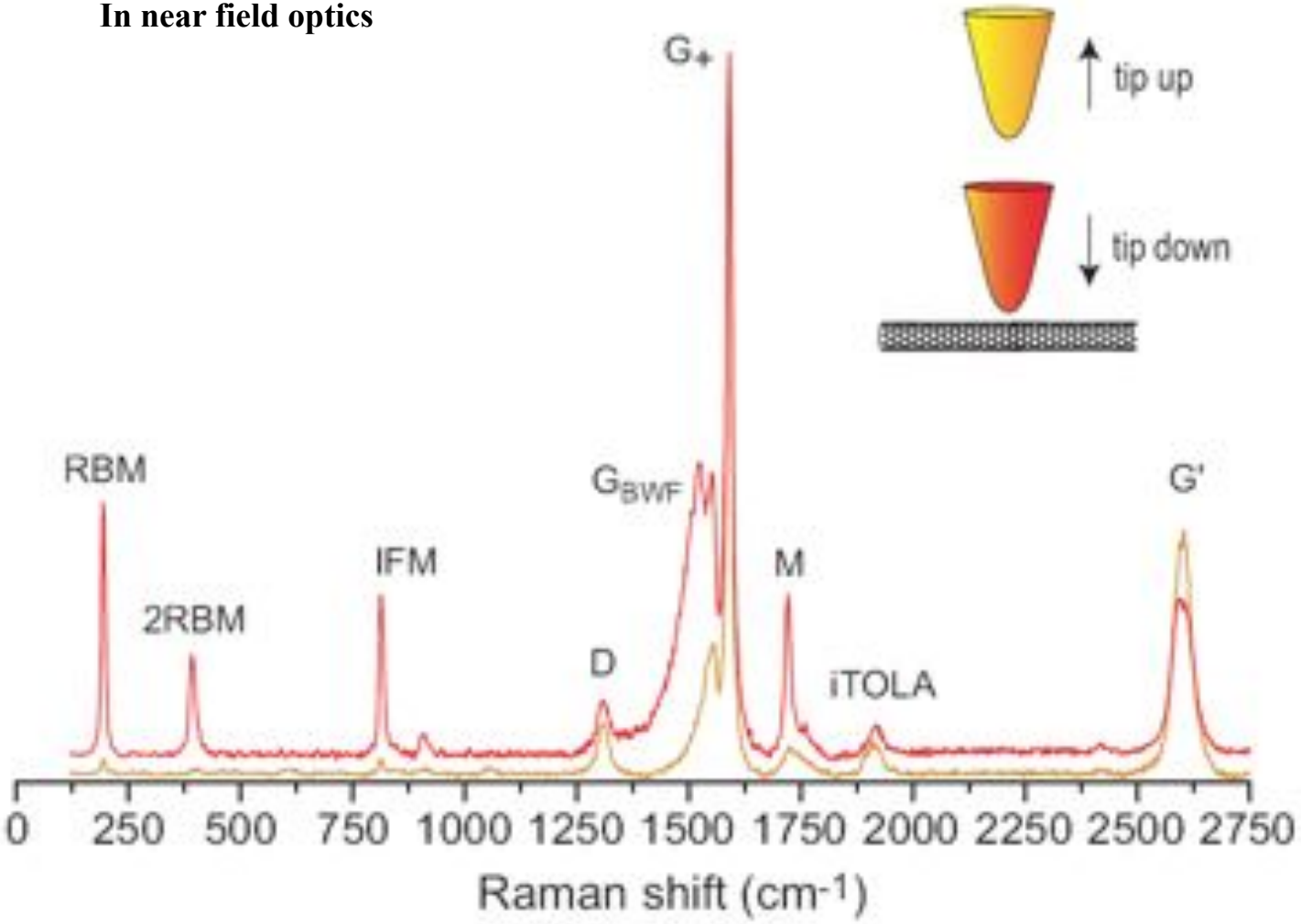

L.G.Cancado, unpublished work

Graphene Ribbons

Zigzag

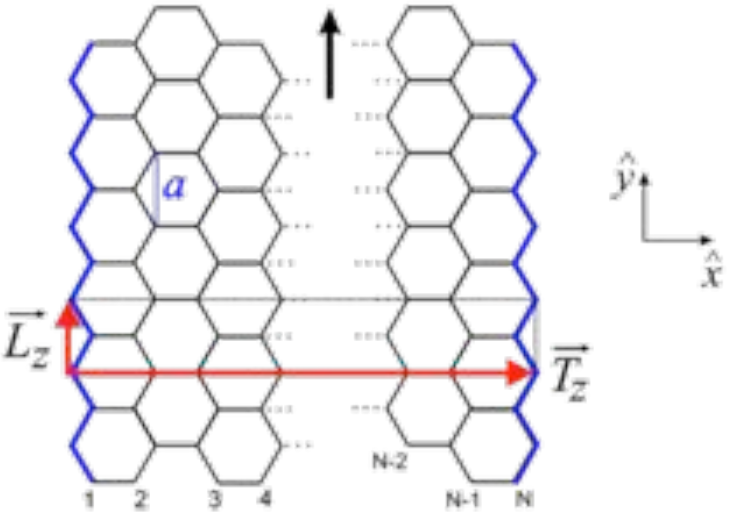

Armchair

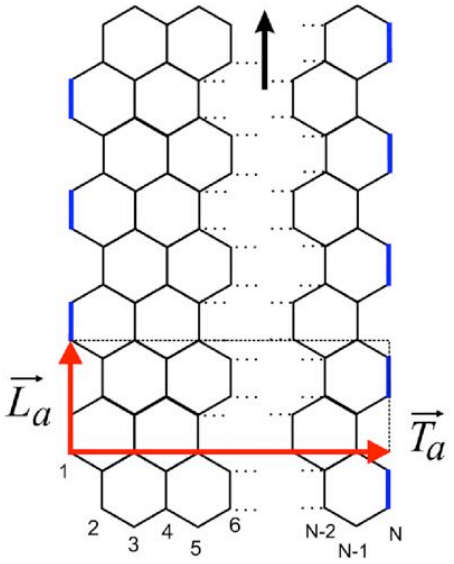

Direction of cutting lines

- Special feature of graphene ribbons is that they have edges and few columns of carbon atoms along the width.

Electronic structure of graphene ribbons

Armchair

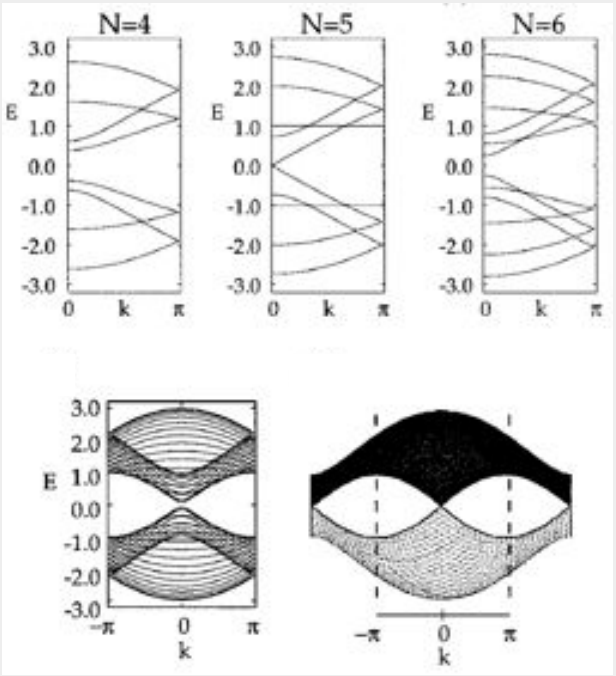

Metallic for N=3M-1 (M integer)
Semiconducting for N=3M& 3M-2
Examples:
Metallic for N=5
and Semiconducting for N=4, 6

Zigzag

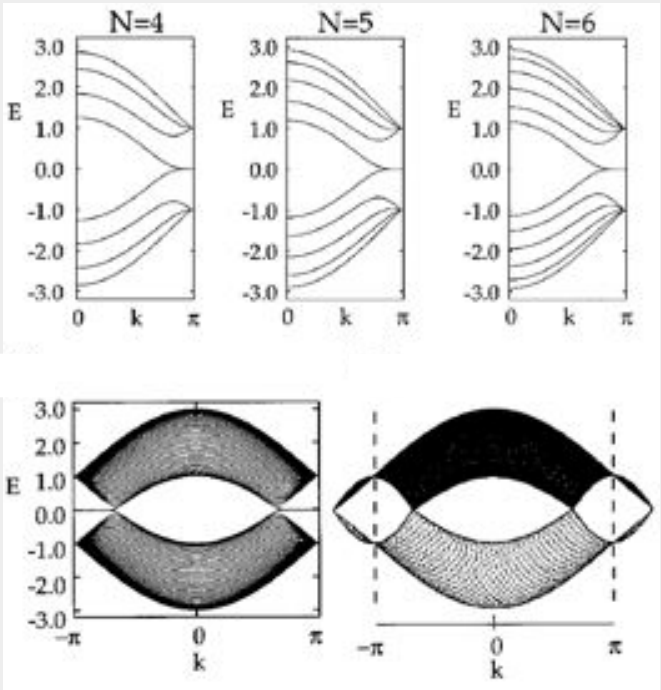

- **Always metallic**
- **Presence of localized edge states at the Fermi level**

Van Hove singularities in the DOS

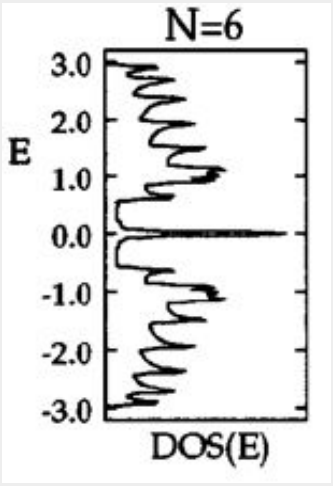

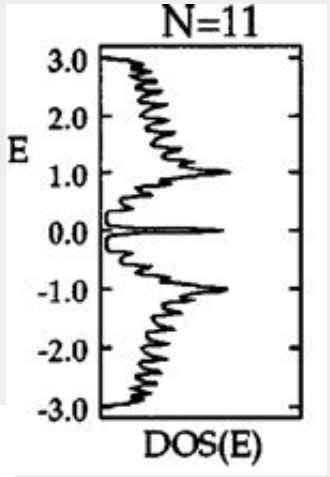

Nakada *et al.*, Phys. Rev. B **54**, 17954 (1996).

Unique Properties of Graphene Nanoribbons

Zigzag

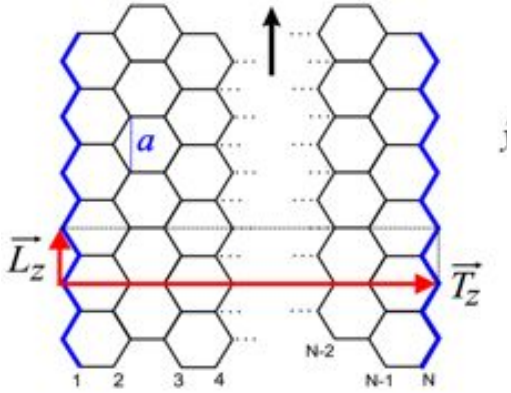

Armchair

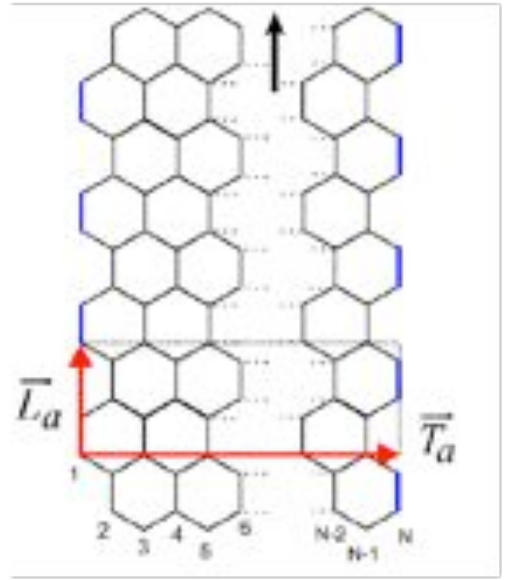

- A special feature of graphene ribbons is their long edges with narrow widths

- The crystallographic orientation of the edges strongly influences their electronic and other properties.

- Zigzag ribbons show a high density of states at E_F and are zero gap semiconductors.

- Armchair edge ribbons (like single wall carbon nanotubes) can be either metallic (N=3M-1) or semiconducting (N=3M, N=3M +1), where N,M are integers

N=number of hexagon columns along the ribbon width.

Raman structure used to Identify graphene nanoribbons

AFM image of many graphene nanoribbons parallel to each other:

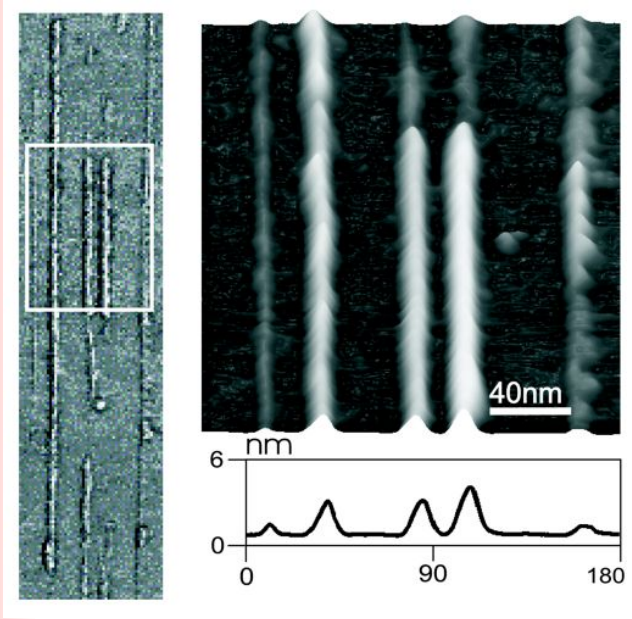

AFM image of a graphene nanoribbon:

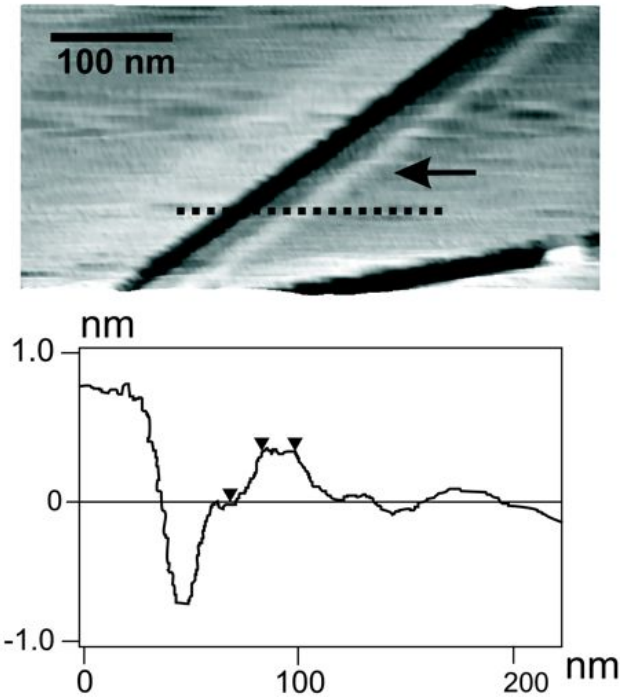

STM image of a zigzag ribbon:

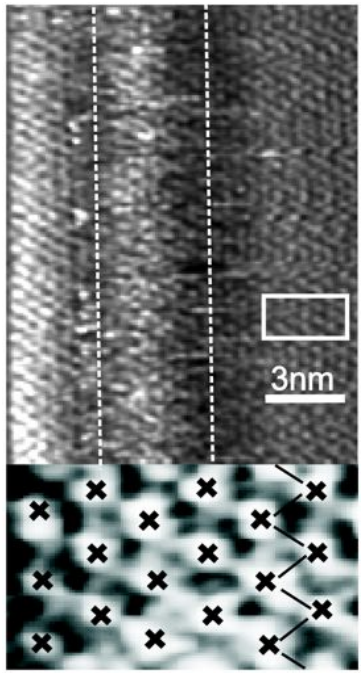

Cançado *et al.*, Phys. Rev. Lett. **93**, 047403 (2004).

Synthesis:

- **Electrophoretic deposition of nano-diamond particles on a HOPG substrate.**
- **At a HTT of 1600^{0}C, the nano-diamond particles are graphitized, forming nanographite sheets and ribbons.**

Affoune et al., Chem. Phys. Lett. **348**, 17 (2001), Langmuir **17**, 547 (2001) .

Raman spectra of graphene nanoribbons

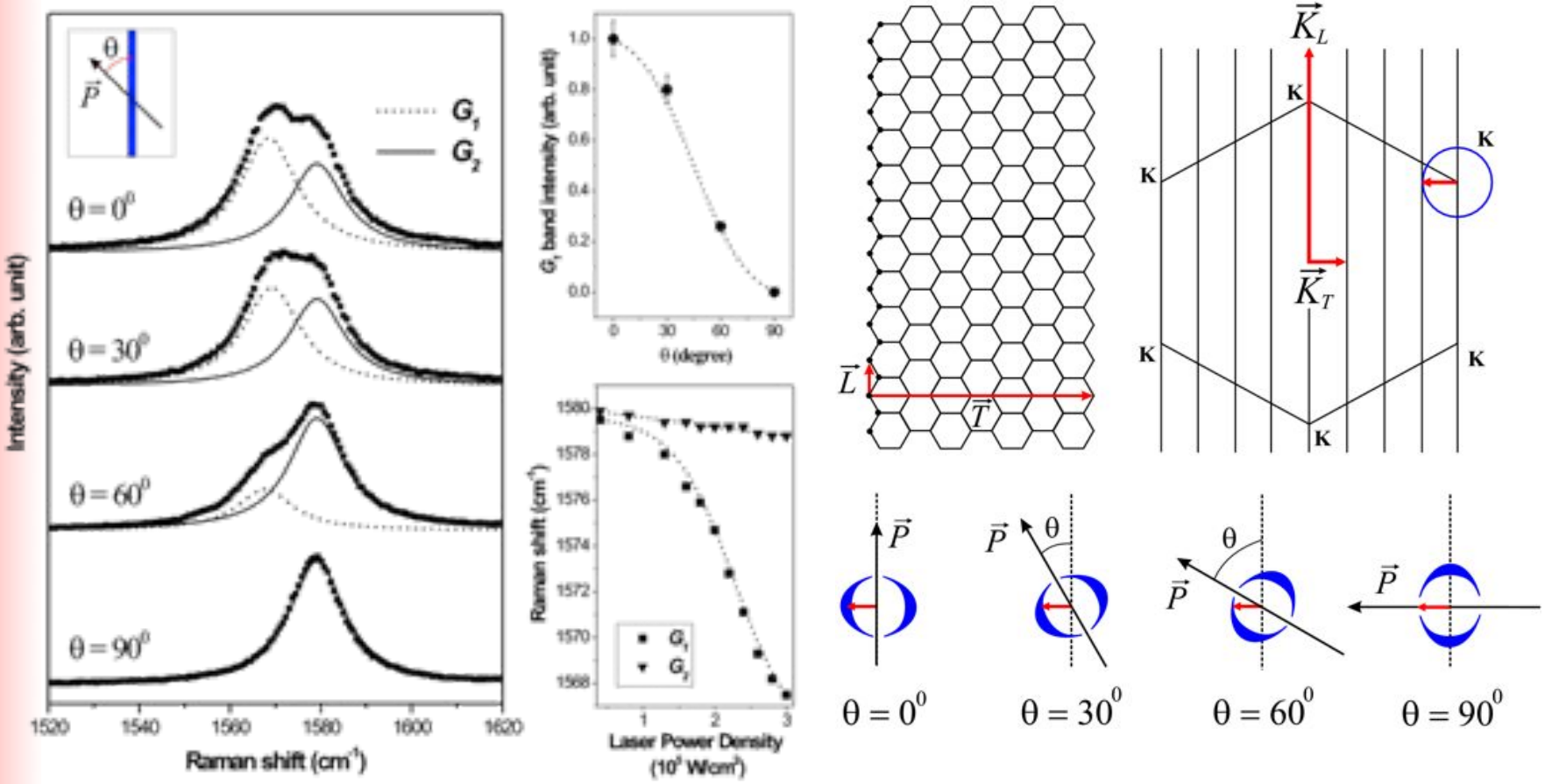

G_1 - graphene nanoribbon
G_2 - HOPG substrate

Cançado *et al.*, Phys. Rev. Lett. **93**, 047403 (2004).

$$W(\vec{k}) \propto \left|\vec{P} \times \vec{k}\right|^2$$

Gruneis *et al.*, Phys. Rev. B **67**, 165402 (2003).

Influence of the atomic structure in the Raman spectra of graphite edges

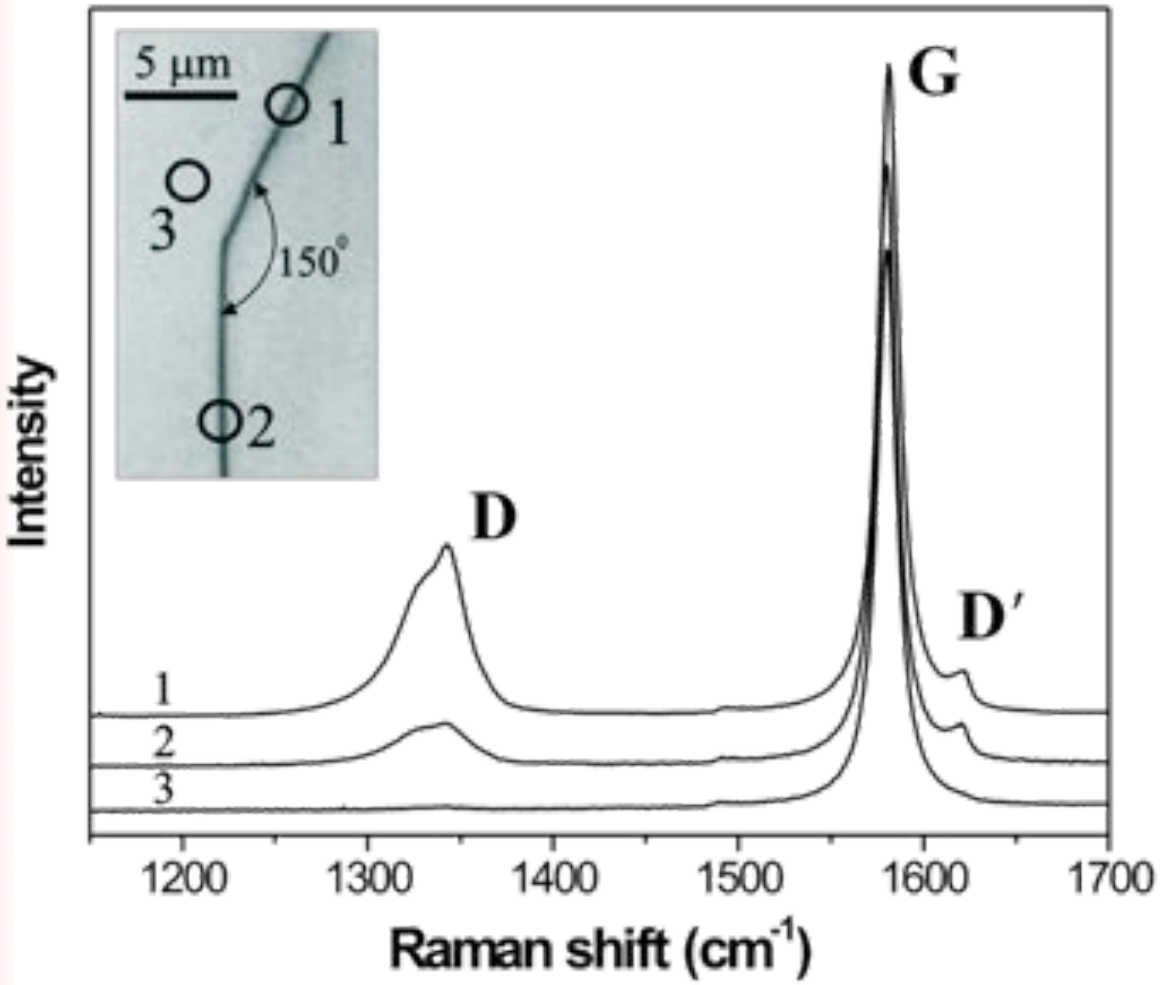

$$I_{D1} > I_{D2}$$
$$I_{D'1} \sim I_{D'2}$$

Cançado *et al.*, Phys. Rev. Lett. **93**, 247401 (2004).

Influence of the atomic structure in the Raman spectra of graphite edges

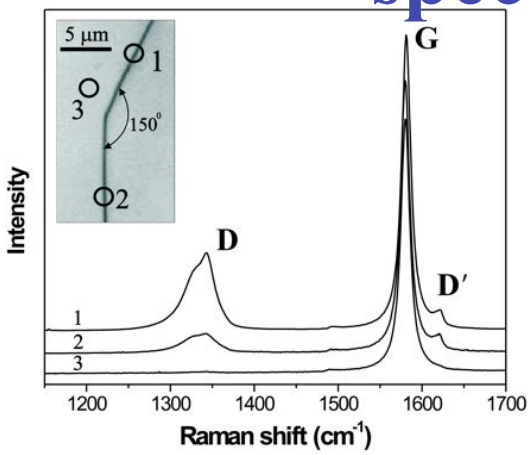

Edge 1:
Armchair

Edge 2:
Zigzag

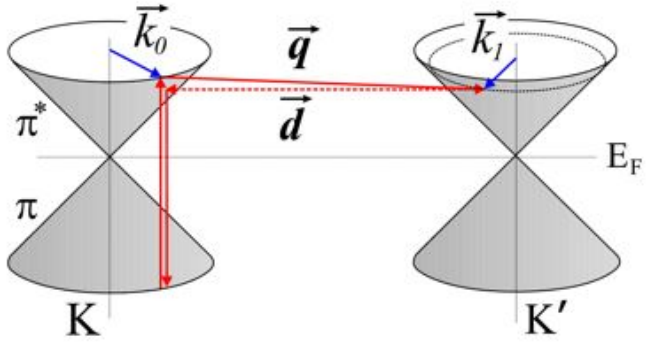

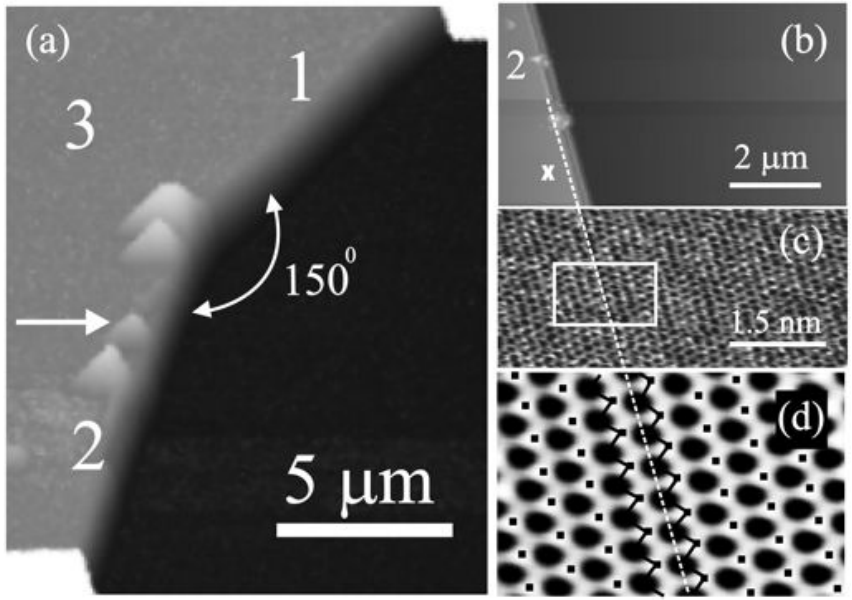

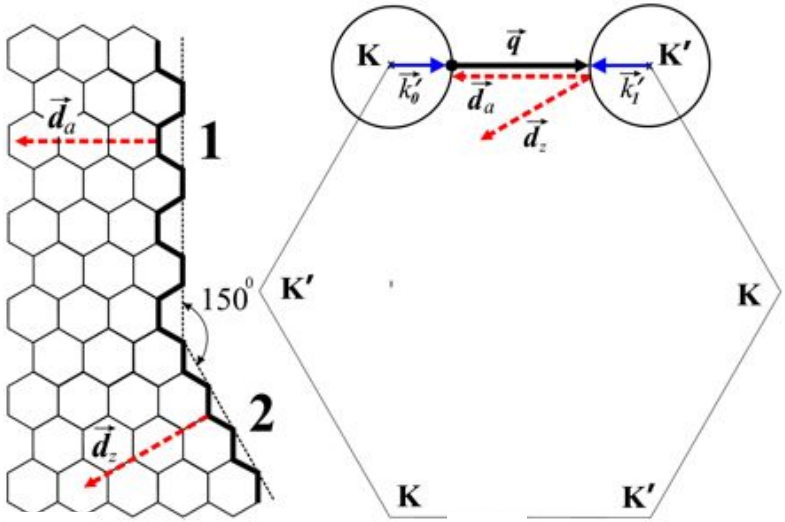

Cançado *et al.*, Phys. Rev. Lett. **93**, 247401 (2004).

The ***D*** band Raman spectra are used to distinguish between armchair and zigzag edges

Outline

- Historical Graphene to Graphene path
- Carbon Nanotubes as Prototype Materials
- Disordered Graphite
- Graphene and Graphene Ribbons
- Looking to the Future of Carbon Nanostructures

Outlook

- 1D carbon nanotubes continue to be an expanding field, now focusing more heavily on applications
- 1D carbon nanoribbons is a newly emerging field that is expected to grow rapidly in the near future, particularly if higher quality ribbons can be made.
- The synergy between nanotubes, graphene and nanoribbons will surely enrich one another strongly in advancing both their nanoscience and applications.

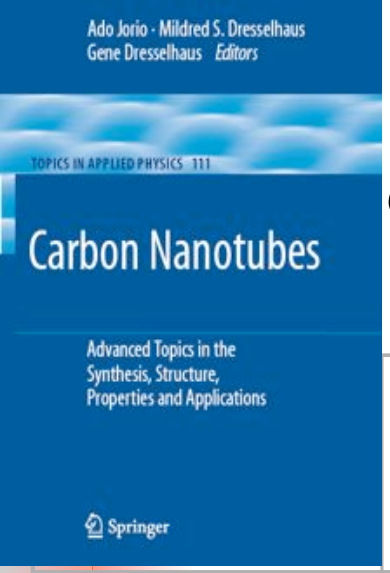

More emphasis now is on applications

Potential Applications of Carbon Nanotubes

Chapter by M. Endo, M. S. Strano, P. M. Ajayan @ Springer TAP111

	Large Volume Applications	**Limited Volume Applications (Mostly based on Engineered Nanotube Structures)**
Present	- Battery Electrode Additives (MWNT) - Composites (sporting goods; MWNT) -Composites (ESD* applications; MWNT) -(*ESD – Electrical Shielding Device)	- Scanning Probe Tips (MWNT) - Specialized Medical Appliances (catheters) (MWNT)
Near Term (less than ten years)	- Battery and Super-capacitor Electrodes - Multifunctional Composites - Fuel Cell Electrodes (catalyst support) - Transparent Conducting Films - Field Emission Displays / Lighting - CNT based Inks for Printing	- Single Tip Electron Guns - Multi-Tip Array X-ray Sources - Probe Array Test Systems - CNT Brush Contacts - CNT Sensor Devices - Electro-mechanical Memory Device - Thermal Management Systems
Long Term (beyond ten years)	- Power Transmission Cables - Structural Composites (aerospace and automobile etc.) - CNTs in Photovoltaic Devices	- Nano-electronics (FET,Interconnects) - Flexible Electronics - CNT based bio-sensors - CNT Fitration/Separation Membranes - Drug-delivery Systems

Outlook

- 1D carbon nanotubes continue to be an expanding field, now focusing more heavily on applications
- 1D carbon nanoribbons is a newly emerging field that is expected to grow rapidly in the near future, particularly if higher quality ribbons can be made.
- The synergy between nanotubes, graphene and nanoribbons will surely enrich one another strongly in advancing both their nanoscience and applications.

Outlook

- 1D carbon nanotubes continue to be an expanding field, now focusing more heavily on applications
- 1D carbon nanoribbons is a newly emerging field that is expected to grow rapidly in the near future, particularly if higher quality ribbons can be made.
- The synergy between nanotubes, graphene and nanoribbons will surely enrich one another strongly in advancing both their nanoscience and applications.

The End